eng

MDPI

Review

A Review of Segmented Stator and Rotor Designs in AC Electric Machines: Opportunities and Challenges

Bhuvan Khoshoo *, Anmol Aggarwal and Shanelle Foster

Department of Electrical Engineering, Michigan State University, East Lansing, MI 48824, USA; aggarw43@msu.edu (A.A.); hogansha@msu.edu (S.F.)
* Correspondence: khoshoob@msu.edu

Abstract: The use of segmented stator and rotor designs in AC electric machine construction offers several significant advantages, including a high-copper fill factor, increased torque density, improved field-weakening performance, simplified manufacturing processes, and enhanced mechanical strength. Additionally, segmented designs allow for the incorporation of oriented steel—either partially or fully—which exhibits excellent magnetic properties in the rolling direction, resulting in more efficient machine performance. However, lamination segmentation also introduces challenges. Parasitic air gaps between segments and an increased number of cut edges in the assembled stack can alter the magnetic properties of the machine, potentially leading to degraded performance. Furthermore, the use of oriented steel remains complex, as its highly nonlinear magnetic properties vary depending on the direction of the magnetic flux. This paper reviews the widely adopted stator and rotor segmentation techniques available in the literature, discussing their potential benefits and limitations. It also covers key aspects such as popular manufacturing approaches, the impact of segmentation on machine performance, advanced finite-element analysis (FEA) techniques for numerical modeling, and experimental methods for evaluating the performance of segmented stator and rotor constructions in AC machines. By addressing these areas, this work provides a comprehensive resource for machine designers seeking to develop AC machines with segmented stators and rotors.

Keywords: AC electric machines; segmented stator; segmented rotor; core loss; oriented steel; finite-element analysis; electromagnetic measurements

Academic Editors: Iolanda De Marco, Antonio Gil Bravo, Thaiyal Naayagi Ramasamy and Valentina Di Pasquale

Received: 30 October 2024
Revised: 18 December 2024
Accepted: 23 December 2024
Published: 1 January 2025

Citation: Khoshoo, B.; Aggarwal, A.; Foster, S. A Review of Segmented Stator and Rotor Designs in AC Electric Machines: Opportunities and Challenges. *Eng* **2025**, *6*, 7. https://doi.org/10.3390/eng6010007

1. Introduction

Over several decades, the demand and utilization of electric machines have continuously expanded. In 2017, US DRIVE (Driving Research and Innovation for Vehicle efficiency and Energy sustainability) Partnership released a roadmap focusing on the cost and size of electric motors for future electric vehicles. The electric motor targets for 2025 include an ambitious 50 kW/L power density while costing only 3.3 USD/kW [1]. In the European Union, electric machines are consuming more than 50% of electricity off the grid, with a steady increase expected in the future consumption [2]. In the last two decades, several alternating current (AC) machine topologies have been investigated for different applications, such as permanent magnet synchronous machines (PMSMs), synchronous reluctance machines (SynRMs), and switched reluctance machines (SRMs). Naturally, the research focus has been on finding solutions for improving the design and controls of motors and associated power electronics components for increasing the torque density, improving production efficiency, and increasing reliability [3–14].

The segmentation of electrical steel lamination can be an effective strategy to achieve these objectives and more, as shown in Figure 1. Segmented stator and rotor designs have been explored in the past for various applications such as domestic appliances, automobiles, more electric aircraft, and power generation [15]. Using segmented lamination can improve the overall manufacturing process as it helps reduce the material waste and, therefore, the material cost, compared to the conventional manufacturing method where both rotor and stator lamination are punched out of the same sheet [16–18]. In large PMSMs, such as the ones used in large grid-connected wind turbines, the segmentation of stator and rotor lamination can help ease the transportation and assembly process as the entire assembly can weigh several tons [19,20].

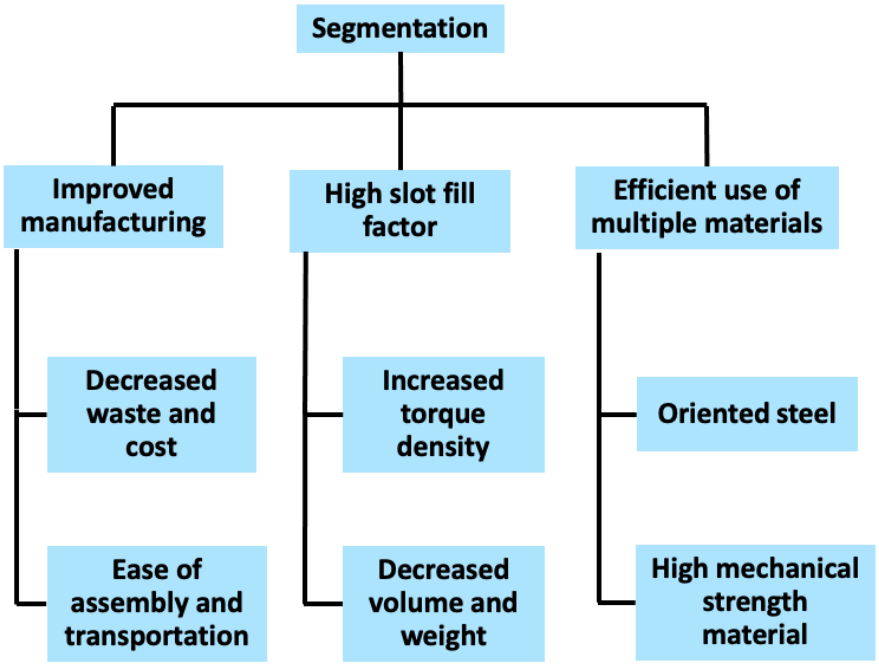

Figure 1. Advantages of using segmented stator and rotor designs over conventional designs.

Segmented stator lamination with a concentrated winding scheme can help achieve a significantly high slot fill factor compared to conventional laminated structures [21]. An increased slot fill factor helps increase the torque density of the machine for the same dimensions. On the other hand, for the same ratings, the motor volume and weight can be decreased. Naturally, segmented stator laminations have been employed in fractional-slot concentrated winding (FSCW) machines. It is shown that using a segmented stator structure can increase the copper fill factor up to 75% [22]. More recently, a particular coil design named maximum slot occupation (MSO) has been reported to achieve as a slot fill factor high as 80% with a segmented stator structure [23]. Segmented stator structures in FSCW machines can also improve the working harmonic and reduce the other sub-harmonics leading to increased torque density and efficiency [24,25].

During high-speed operation, the stator experiences high-frequency magnetic flux, leading to significant core loss, while the rotor must endure mechanical stress to maintain structural integrity. Consequently, the material requirements for stator and rotor construction differ. To reduce core loss, thinner laminations are preferred, whereas thicker laminations enhance structural integrity. Certain materials, such as Hi-Lite ultra-thin gauge electrical steel [26], are optimized to balance these conflicting demands and are suitable for manufacturing soft magnetic cores. However, separately punching stator and rotor laminations from different materials [27], combined with segmentation, offers greater flexibility

in electric machine construction. Using oriented steel in the stator core improves average torque and reduces core loss due to its superior magnetic properties in the rolling direction compared to nonoriented steel [28–30]. Similarly, materials with higher mechanical strength can be used for rotor laminations. This separate punching approach also allows for tighter manufacturing tolerances on air gap length, enhancing air gap flux density and enabling more torque-dense machines [29].

Faults may lead to adverse effects on the operation of the machine and are dangerous to the system and to human safety [31–35]. As a result, fault-tolerant machine designs are preferred in safety-critical applications. Single-layer FSCW (SL-FSCW) winding is inherently more fault-tolerant than other winding types, as the impact of one phase on another is minimized. In modifying the stator to be segmented, the assembly can be simplified. Moreover, the replacement of the damaged parts post fault becomes easier, which makes them favorable for fault-tolerant and safety-critical applications [36–40].

Although there are several advantages of using segmented stator and rotor designs in PMSMs, there are several challenges associated with doing so as well, as shown in Figure 2. Segmentation introduces a physical gap between two adjacent segments, which cannot be reduced to zero due to manufacturing accuracy limitations. These nonzero air gaps change the magnetic circuit of the machine and can have significant impact on the electromagnetic performance. It has been shown that additional flux gaps due to segments can significantly increase the cogging torque and decrease the amplitude of the working harmonic leading to decreased magnet torque [41,42]. Using segmented stator can also lead to reduction in the resonance frequency of the natural vibrational modes of the stator, increasing the probability of exciting the natural modes compared to the conventional stator structure [43]. Therefore, machine designers must carefully select the number of segments in addition to the slot/pole combination to ensure suitable NVH performance of the machine [44].

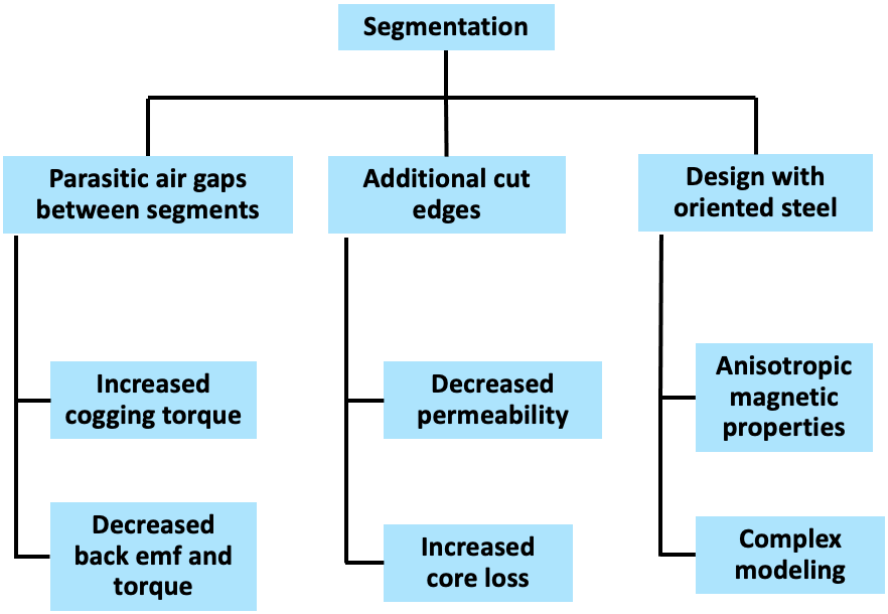

Figure 2. Drawbacks of using segmented stator and rotor designs.

The finite-element modeling of segmented stator and rotor designs also presents several challenges. The egmentation of lamination introduces additional cut edges into the assembled core. It has been shown that the magnetic properties significantly degrade around the cut edges present in electrical steel lamination [45,46]. Consequently, a segmented soft magnetic core with additional cut edges will lead to increased core loss compared to a conventional core [29,47]. However, conventional finite-element analysis (FEA) software

inherently does not consider the impact of cut edges during core loss calculations. Therefore, the existing methods must be modified, and local magnetic properties as a function of distance from the cut edge should be used for more precise core loss calculations [45,48].

While the use of oriented steel in segmented stator and rotor structures is popular for improving motor performance, the design process is challenging due to its anisotropic magnetic properties. Conventionally, the modeling of oriented steel in most commercial FEA tools is realized using an elliptical model [49] that requires BH curves in the rolling and the transverse directions. The magnetic properties for all other directions, between 0° (rolling direction) and 90° (transverse direction), are interpolated using analytical or spline functions. However, the FEA interpolation of magnetic properties is not accurate, and the worst magnetic properties are not observed in the transverse direction, but rather close to 55° away from the rolling direction [50,51]. As a result, the accurate modeling of oriented steel remains an important topic for the electric machines community.

With recent advances in additive manufacturing, segmented stator and rotor structures can open pathways to more complex and unprecedented designs to meet the challenges associated with the cost and sizing of future electric machines. This work provides the most comprehensive information on segmented stator and rotor designs. Section 2 presents different manufacturing techniques for segmented stator and rotor cores. Section 3 discusses the impact of stator and rotor segmentation on the electromagnetic performance of segmented designs. Section 4 expands on the impact of additional cut edges that are inevitable in segmented stator designs. Section 5 explores motor performance enhancement with oriented steel and discusses the FEA modeling of segmented stators manufactured using oriented steel. Section 6 summarizes the conclusions of this paper and outlines potential research opportunities to address current gaps.

2. Manufacturing Techniques for Segmented Stator and Rotor Cores

The manufacturing methods for segmented stator and rotor cores predominantly depend on the available resources and final cost. Broadly, these methods can be divided into two parts: (1) manufacturing using conventional tools and (2) manufacturing using special tools. Different methods have different impacts on the punching waste, production efficiency, and machine performance [18,52]. Methods involving conventional tools include punching separate lamination segments and then joining them together to form the complete core. Using special tools, such as manufacturing using rolled out stator segments, can lead to an easier assembly process compared to conventional methods [18].

2.1. Manufacturing Using Conventional Tools

For a soft magnetic core made using conventionally punched segments, the complete manufacturing cycle involves two steps: the (1) punching of individual segments and (2) assembly of punched segments to form a complete core. For modular stator cores with a concentrated winding scheme, each stator tooth can be punched separately to significantly decrease the punching waste and increase the copper fill factor. In MW-scale PM machines, single-tooth punching can provide other benefits including lightweight construction, the ease of transportation and assembly, and the use of common modules for all specifications [20,53]. For distributed winding machines, the choice of the number of segments is influenced by the slot/pole combination of the machine. Since segmentation introduces flux gaps between two segments, an improper selection of the number of segments can lead to imbalanced magnetic circuits, which can introduce significant torque ripple [54]. An example of punched segments for a concentrated winding [55] and a distributed winding [15] machine are shown in Figure 3 and Figure 4, respectively.

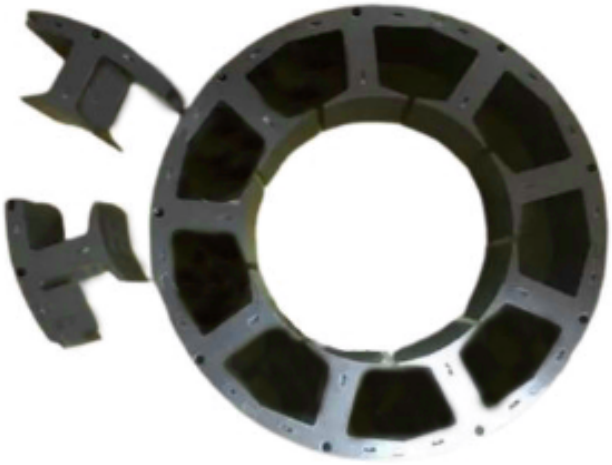

Figure 3. Segmented stator cores for concentrated winding scheme [55].

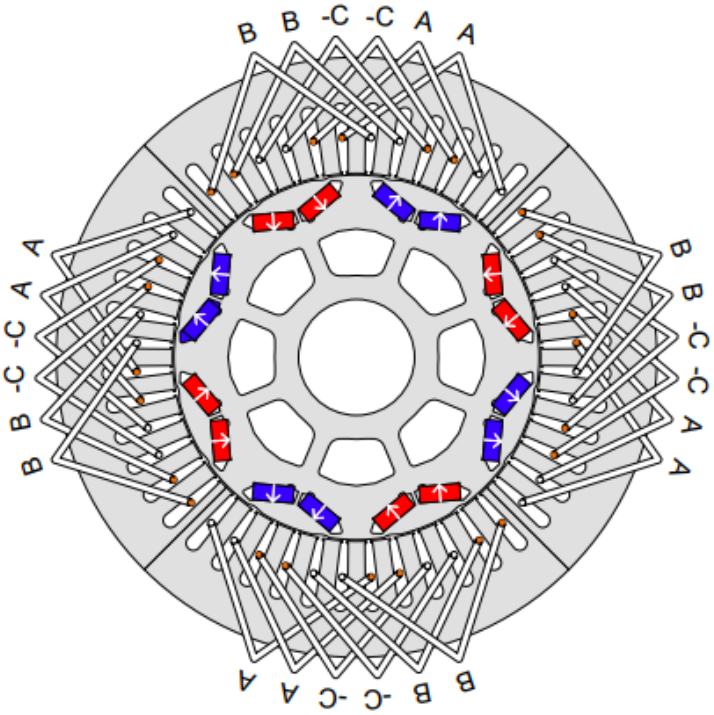

Figure 4. Segmented stator core for distributed winding scheme [15].

After punching the individual lamination segments, the assembly process is completed in two steps: the (1) assembly of individual segments to form a segmented stack and (2) assembly of multiple segmented stacks to form a complete stator or rotor core. Both these steps can involve using either one or a combination of multiple techniques, which can be classified into three categories [56]: (1) welding, (2) interlocking, and (3) bonding.

2.1.1. Welding

Welding is a cost-efficient and fast-moving method used to join separately punched segments and assemble segmented stacks to form a complete core [27]. However, welding can significantly increase the core losses of the assembled core due to the local degradation of magnetic properties at the weld joint [57]. Nevertheless, for prototype samples and some applications with large torque requirements, where the stack tolerances are not very strict, welding still remains the preferred method [56]. It must be emphasized that

the deterioration of the material properties at the weld joint is highly dependent on the welding technique.

2.1.2. Interlocking

Interlocking requires punching segments with a projecting element on one edge and a compatible receptive element on the other edge. To join individually punched segments to create a segmented stack, each lamination segment is pressed down into the one underneath it by forming tiny depressions. These depressions keep the segmented stack together. Different interlocking shapes have been studied in the literature [58–60], as shown in Figure 5. Out of the three types of interlocking structures shown here, the Omega-shape interlock is considered the optimal choice for the segmented stator design due to the lower negative impact on the electromagnetic performance and easier processing and assembly compared to the Trapezoid- and T-shape connections [59]. The practical implementations of Trapezoid-shape and Omega-shape interlocking shapes are shown in Figures 6 and 7, respectively. For circumferentially segmented rotor designs with magnets, interlocking is combined with a brick wall design [16,17], where segments belonging to every alternate layer in the axial direction are shifted with an offset angle, as shown in Figure 8. This particular design also allows us to transfer and distribute the mechanical forces to the contact surface between the magnet and the magnet slot.

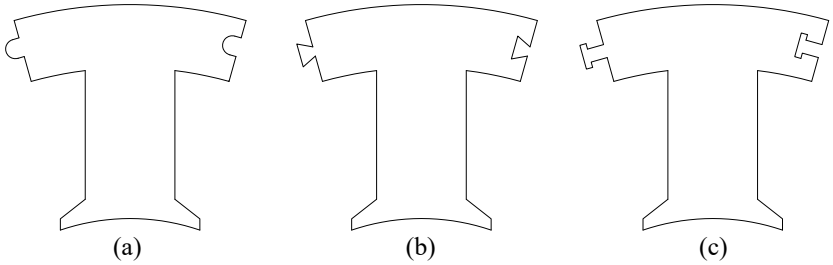

Figure 5. Suggested shapes of interlocking structures: (**a**) Omega-shape, (**b**) Trapezoid-shape, and (**c**) T-shape. Figures adapted from [59,60].

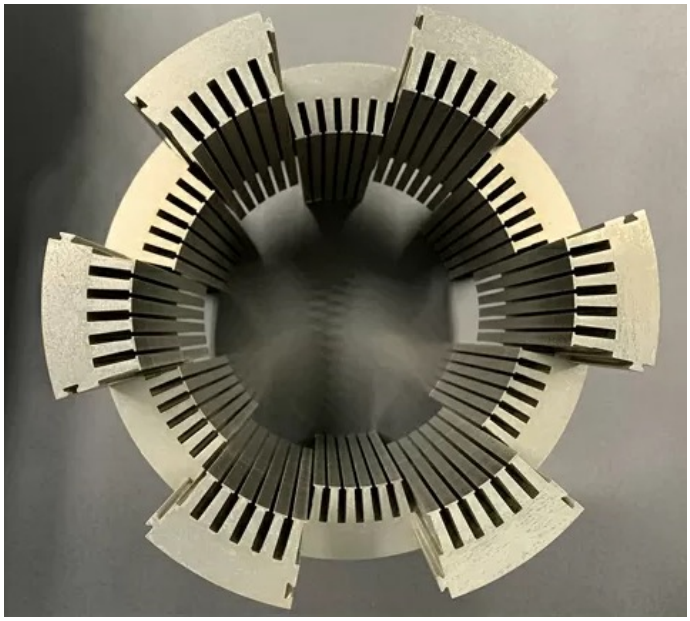

Figure 6. Segmented stator stack with Trapezoid-shape interlocking feature [61].

Figure 7. Segmented stator stack with Omega-shape interlocking feature [55].

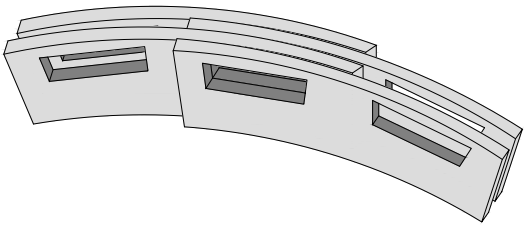

Figure 8. Brick wall design for joining circumferentially segmented rotor lamination. Figure adapted from [17].

Although interlocking is a highly productive assembly method with easy stack handling, there are certain practical limitations associated with it. The tiny depressions formed during the formation of an individual segmented stack can lead to shorted layers and increased eddy current losses. Moreover, for high-speed operation, it is common practice to decrease the lamination thickness to control the eddy current losses. However, using very thin steel sheets makes it difficult to form these depressions, which can fail to generate the required joining forces [27]. In such cases, interlocking can be supplemented with welding to securely assemble an individual segmented stack. Moreover, it is common practice to use a tight stator frame or a press fit to join multiple segmented stacks with interlocking connections [15]. In some cases, the segmented stator core assembly may include radially segmented teeth and back iron instead of a circumferential segmentation. Joining such segments may require using either a press fit or special dovetailed connections to provide adequate stiffness for withstanding the radial magnetic forces [29], as shown in Figure 9. Similar examples of dovetailed connections being used for assembling segmented rotor structures can also be found in the literature [62–64]. Using press-fit or dovetailed connections leads to high compressive stress at the connection interface, which can have significant negative impact on both hysteresis and eddy current losses [57,65].

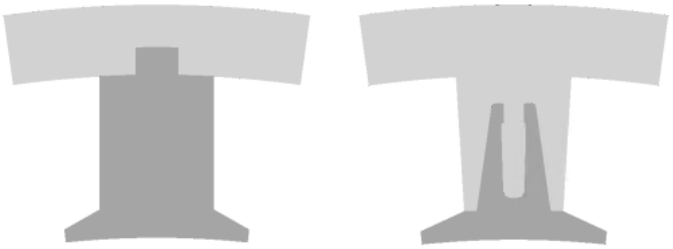

Figure 9. Interlocking shapes used for radially segmented stator tooth and back iron structures [29].

2.1.3. Bonding

The bonding operation involves joining two parts using some form of adhesive or glue at the joining surfaces of those parts. There are two main bonding technologies used by manufacturers: (1) dotted bonding and (2) full-face bonding [27]. Compared to dotted bonding, full-face bonding applies adhesive on the entire available surface area and provides high structural stability even with very fine stack tolerances. Bonding also allows the use of very thin steel sheets with more intricate shapes and provides greater flexibility in overall manufacturing. In [66], the effect of using bonding on assembling a segmented stator was explored. Two segmented stator prototypes are manufactured: (1) P1 made from 0.35 mm thick laminations, which are held together using notching and a stainless steel compression band, and (2) P2 made using 0.1 mm thick laminations, which are glued together without any punch feature. Naturally, the selection of thinner laminations leads to more than a 15% decrease in the iron loss in segmented stator P2 compared to P1. Nevertheless, current bonding technologies suffer from high costs and longer assembly time. More details about bonding technologies are discussed in [67]. A summary of the the three conventional assembly methods is presented in Table 1.

Table 1. Comparison of different assembly methods for manufacturing using conventional tools.

Assembly Method	Advantages	Limitations
Welding	Fast-moving, cost-efficient	Local degradation at weld joint
Interlocking	High productivity, easy stack handling	Use of very thin sheets, additional press fit
Bonding	Use of very thin sheets, manufacturing flexibility	High cost, longer assembly time

2.2. Manufacturing Using Special Tools

Depending on the size and slot/pole combination of the machine, conventionally punched lamination segments can significantly increase the total number of components. This can lead to a difficult assembly process due to the accumulation of errors involved with individual component processing. To avoid these drawbacks, alternate methods have been proposed in the literature. In [68], the author suggests using a long iron band and punching the lamination segments in a side-by-side fashion, where the adjacent segments are not entirely separate but connected via a rotating joint, as shown in Figure 10.

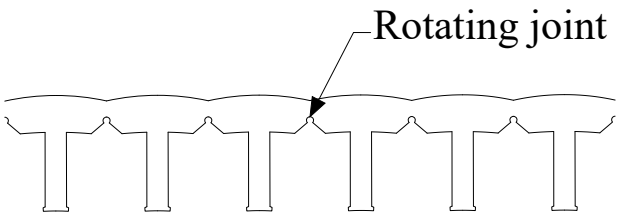

Figure 10. Partially connected lamination segments punched using a long iron band.

These partially connected segments can be rolled in form of a spiral core (see Figure 11) and held together using welding. However, such methods may not be suitable for machines with a large back iron thickness, which makes rolling the iron band difficult [18]. Moreover, the assembled lamination are in a mechanical state of plastic deformation and residual elastic stress, which can lead to deteriorated magnetic properties [69]. Another method involving a joint-lapped core structure is suggested in [22], where the segments are punched out of a long iron band, with concave- and convex-shaped joints on the front and back sides.

These joints are then overlapped to form a rotation axis and can be assembled to form a complete core. The joint-lapped core assembly can eliminate the restrictions due to winding nozzle orbit and improve the copper fill factor compared to the spiral core assembly [22]. Several similar methods have been presented in the literature [70–72]. Nevertheless, all such manufacturing methods require special machine-specific production tools, which can end up increasing the cost of production.

Figure 11. Spiral core assembly [73].

3. Electromagnetic Performance of Segmented Designs

Segmented stator and rotor designs introduce parasitic gaps, which are tough to eliminate due to manufacturing limitations. Different segmentation types lead to different impacts on electromagnetic performance, as discussed below.

3.1. Segmented Stator Designs

The two most prevalent segmented stator designs involve segmentation along the (1) stator slot and (2) stator tooth, as shown in Figure 12 and Figure 13, respectively.

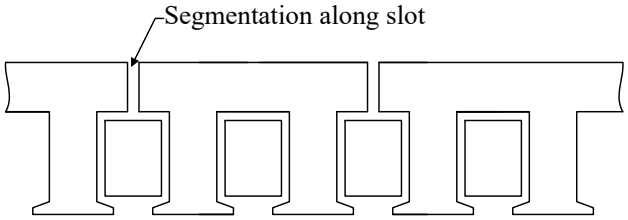

Figure 12. Segmented stator design with segmentation along the stator slot.

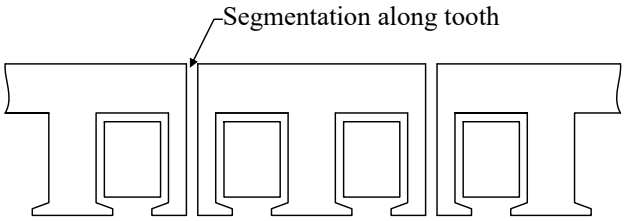

Figure 13. Segmented stator design with segmentation along the stator tooth.

3.1.1. Segmentation Along the Stator Slot

Segmentation along the stator slot can increase the slot fill factor and, therefore, the average torque of an electric machine. Naturally, segmentation along the slot is popular with a single-layer fractional slot concentrated winding (SL-FSCW) schemes, where each wound tooth can be an individual segment to maximize the slot fill factor and ease the winding assembly [21,66]. The utilization of a segmented stator design in machines with a distributed winding scheme is limited, mostly due to overlapped winding. In such cases, stator segmentation can lead to increased end winding connections and copper loss [15].

Despite the advantages seen in the slot fill factor, a segmented core introduces additional air gaps between two adjacent segments, which change the magnetic circuit of the machine. The influence of such parasitic gaps has been extensively analyzed [41,74–77]. The presence of parasitic gaps has shown to increase the cogging torque of the segmented machine, with the effects becoming more severe for larger or non-uniform gaps [41]. Additionally, the increased reluctance due to parasitic gaps decreases the back-emf and, therefore, average torque of the machine. It is also shown that for machines with distributed winding schemes, the selection of number of segments for satisfactory performance is dependent on the number of slot/pole combination and number of poles per segment [75]. Moreover, the parasitic gaps can also increase the flux leakage through adjacent tooth tips due to an increase in the material saturation [76].

3.1.2. Segmentation Along the Stator Tooth

Segmentation along the stator tooth is not as popular as segmentation along the slot, since the winding nozzle orbit is restricted and there is no benefit observed in the slot fill factor of the machine. However, regardless of the parasitic gaps, such a segmentation technique has the potential to increase the average torque by improving the winding factor of the machine. Although such designs have been studied with double-layer FSCW (DL-FSCW) winding schemes [78,79], single-layer FSCW designs have been investigated more due to their enhanced fault tolerance. The two possible segmented designs with single-layer winding, FSCW-FB1 and FSCW-FB-2, are shown in Figure 14a and Figure 14b, respectively. Here, each unwound tooth is radially segmented for FSCW-FB1, while each wound tooth is segmented for the FSCW-FB2 design. From a construction point of view, FSCW-FB1 piques more interest, as each segmented stack can be wound individually before the final assembly. On the other hand, FSCW-FB2 requires assembling the stator core first to allow the winding assembly.

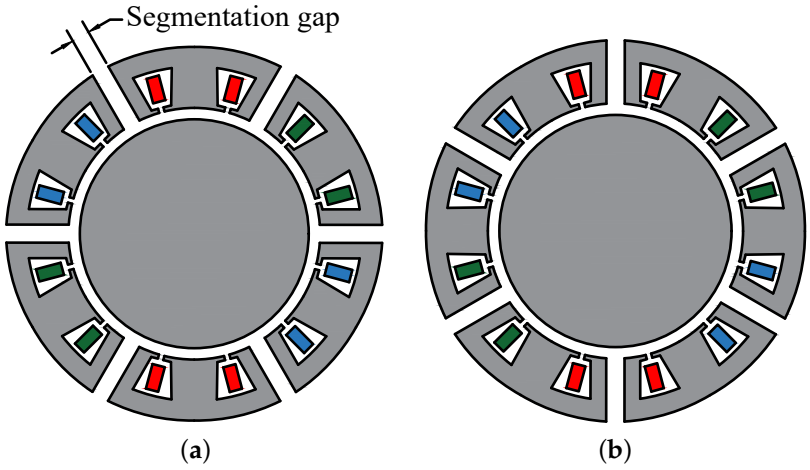

Figure 14. Examples of stator segmentation along the tooth with a single-layer concentrated winding scheme. (**a**) FSCW-FB1—each wound tooth is a segment. (**b**) FSCW-FB2—each unwound tooth is a segment.

Segmented stator machines with the FSCW-FB1 design have been analyzed extensively in [24,25,40,42,78,80–83]. Dajaku showed in [24,25] that placing flux barriers in the stator tooth region decreases the fundamental sub-harmonic while increases the working harmonic of the stator MMF. It is shown that the FSCW-FB1 design decreases the flux linkage and winding factor of machines with $N_s > 2p$, while it increases the flux linkage and winding factor of machines with $N_s < 2p$, where N_s and $2p$ represent the number of stator slots and number of rotor poles, respectively [42]. In [81,82], the performance of

a 12-slot/14-pole FSCW-FB1 design is compared with its conventional counterpart. It is shown that the FSCW-FB1 design decreases the fundamental and the fifth harmonic but increases the seventh harmonic of the stator MMF, which is also the working harmonic for a 12-slot/14-pole PM machine. Under the same electrical and geometric constraints, the segmented machine generates more torque with lower rotor iron and magnet losses leading to an overall increase in torque density and efficiency. Overall, the FSCW-FB1 design is suitable for machines with $N_s < 2p$ but should be avoided for machines with $N_s > 2p$.

The impact of the FSCW-FB2 design on the winding factor of a 12-slot/10-pole machine is explored in [84] using the stator current linkage theory. It is shown that by introducing flux gaps, additional voltage phasors are generated in the flux gap, which can be used to calculate an equivalent winding factor. In assuming that the current linkage changes at the middle of the flux gaps, a suitable location of the flux gaps in the stator can be identified for certain slot/pole combinations. The authors systematically showed that for a 12-slot stator, the FSCW-FB2 design can decrease the sub-harmonic winding factor and increase the fifth harmonic winding factor, making it suitable for machines with $N_s > 2p$.

Both the FSCW-FB1 and FSCW-FB2 designs were systematically analyzed in [85–88]. In [85], the authors showed that for the same machine dimensions, using the FSCW-FB1 design in a 12-slot/14-pole and FSCW-FB2 design in a 12-slot/10-pole machine leads to approximately a 10% increase in average torque compared to conventional machines. Thus, for the same rated torque, the machine volume can be decreased leading to increased torque density and efficiency compared to its conventional counterparts. In [86], some important design rules for an appropriate design of FSCW-FB1 and FSCW-FB2 configurations are presented. It is shown that the impact of the flux gaps on the flux linkage distribution can be minimized by placing symmetrical flux gaps, which are equidistant from the positive and negative side of the coil. In [88], the authors compared several different slot/pole combinations for the FSCW machines and verified the usefulness of the FSCW-FB1 and FSCW-FB2 designs for machines with $N_s < 2p$ and $N_s > 2p$, respectively. In [89], a magnetic-equivalent circuit (MEC) model of the radially segmented tooth is presented. Under the assumption of no saturation, the proposed model can accurately capture the impact of parasitic gaps on the magnet flux linkage of machines with different slot/pole combinations. A brief comparison of the two segmented stator topologies is presented in Table 2.

Table 2. Comparison of segmented stator topologies.

Feature	Segmentation Along Slot	Segmentation Along Tooth
Common Applications	SL-FSCW winding	SL- and DL-FSCW winding
Advantages	Improved winding assembly, high slot fill factor	Control of MMF harmonics, improved torque density
Limitations	Nonzero parasitic gaps, increased cogging torque, decreased back-emf	No improvement in fill factor, requires specific slot/pole, complex assembly
Suitability	Best suited for SL-FSCW, limited for distributed winding	FSCW-FB1: $N_s < 2p$, FSCW-FB2: $N_s > 2p$

3.2. Segmented Rotor Designs

The utilization of segmented rotor designs in AC electric machines is dependent on how robust the rotor structure is. Assembling a segmented rotor can present a challenge and the operation at high speed raises further structural integrity concerns. Segmented rotor designs in switched reluctance machines (SRMs) have been extensively investigated, since the rotor is free from magnets and is more robust compared to a PMSM rotor [62,90–93].

3.2.1. Segmented Rotor Switched Reluctance Machines

In early 2000s, a novel segmented rotor construction was presented in [62,90], where the authors investigated the electromagnetic performance of a segmented rotor SRM design to a conventional tooth rotor machine for a 12-slot stator, as shown in Figure 15. Due to shorter magnetic flux paths, the segmented rotor construction increases the flux linking per coil compared to the conventional design. Consequently, the average torque can be increased. In addition, optimizing the stator slot geometry can further improve the performance of the segmented rotor SRM [92]. It must be mentioned that full-pitch winding has to be used for a distributed winding scheme, which can lead to longer end winding connections and increased copper loss compared to a conventional SRM for some designs.

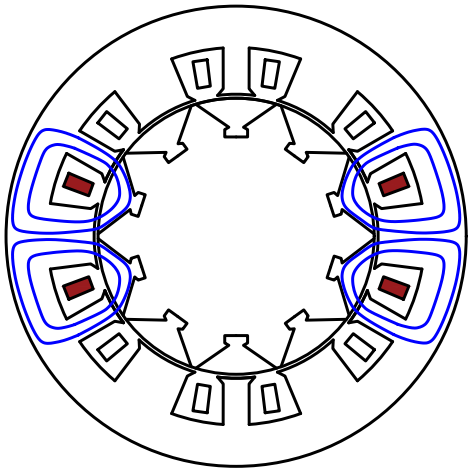

Figure 15. Segmented rotor construction for a 12–10 SRM. Figure adapted from [90].

In [91], the electromagnetic performance of a novel segmented rotor 6–4 SRM was investigated, where the rotor segments were embedded in a solid aluminium rotor hub, as shown in Figure 16. Apart from the increased flux linkage and average torque, the segmented rotor structure provides better distribution of radial forces and decreases the vibrations and acoustic noise compared to the conventional design. However, due to the presence of a nonmagnetic aluminium hub at the air gap, considerable eddy currents are generated in the rotor segments, which can degrade the thermal performance of the machine [94]. Similar segmented rotor construction has been used for the performance improvement of outer-rotor SRMs [95,96].

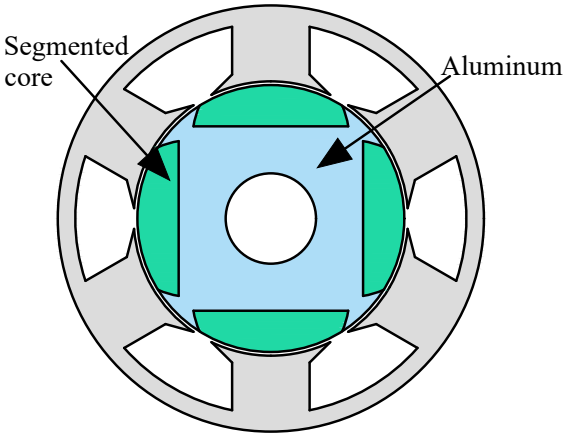

Figure 16. Construction of segmented rotor SRM with solid aluminum block in rotor. Figure adapted from [91].

In [97], a five-step topology modification procedure, based on an energy conversion concept, was introduced to reach a novel segmented rotor design for an SRM. Each step of the procedure focuses on improving the energy conversion capacity of the design to enhance the torque production. In the first step, the windings are rearranged to decrease the end winding length while keeping the same iron volume, leading to decreased copper loss. The second step keeps the same winding arrangement and the iron path length is decreased, which leads to a shorter magnetic flux path. Following this, the air gap radius is increased in the third step, which increases the magnetic pole arc and, consequently, the magnetic loading capacity. In the fourth step, the pole width is decreased to obtain two closed magnetic flux paths per phase winding, which increases the magnetic flux linkage. Finally, two pole teeth in the path of the winding flux maximize the energy conversion capacity in the fifth step. It is worth mentioning that the segmented rotor design used for an SRM can also be used for a flux switching machine (FSM) [98,99], which has been explored to improve the electromagnetic performance compared to the conventional machine [64]. The torque production of a segmented SRM (SSRM) can be further increased using a PM-assisted SSRM (PMA-SSRM) [100,101]. The use of segmented rotor designs has shown to improve mechanical strength, easy assembly, and increased torque density compared to conventional SRMs. Despite these advantages, the SRMs inherently suffer from low torque density and high ripple content and offer limited applications.

3.2.2. Segmented Rotor Permanent Magnet Synchronous Machines

Segmented rotors in PMSMs have been explored relatively less. A primary reason for this lack of attention can be attributed to the question of its practicality, as the rotor assembly becomes challenging. In the late 1990s, segmented rotors in PMSMs were explored to improve the flux-weakening performance of the machine. A novel segmented rotor PMSM is presented in [102,103], where the impact of segmentation along the d-axis was investigated for a spoke-type PMSM, as shown in Figure 17. This placement of flux barriers decreases the saturation of the machine by obstructing armature (q-axis) flux, which provides higher overload performance. However, the current density in the stator has to be increased to maintain rated performance. This configuration also reduces the reluctance torque of the machine. In addition, the considered spoke-type design only allows segmentation along the magnet's d-axis.

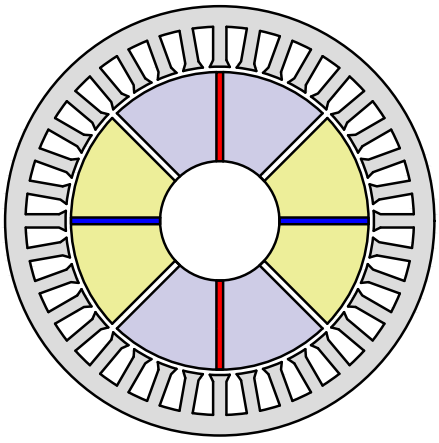

Figure 17. Segmented rotor design with flux barriers along the d-axis. Figure adapted from [102].

A similar idea was explored in [104,105]. Flux barriers are used to obstruct q-axis flux and achieve a higher d-axis inductance (L_d) than q-axis inductance (L_q), as shown in Figure 18. This specific machine type, called a normal saliency permanent magnet (NSPM) machine, can offer better overload performance. It can also provide better field-weakening

(FW) performance, since the machine is mostly operated with a positive or slightly negative d-axis current (I_d), allowing the current vector to be sustained until higher speeds. However, these NSPM machines, further explored in [106], are a specific design, and the analysis is not transferable to other machine topologies. In addition, the design does not employ actual segmentation as the flux barriers do not extend from the rotor's inner diameter (ID) to the rotor's outer diameter (OD), as shown in Figure 19.

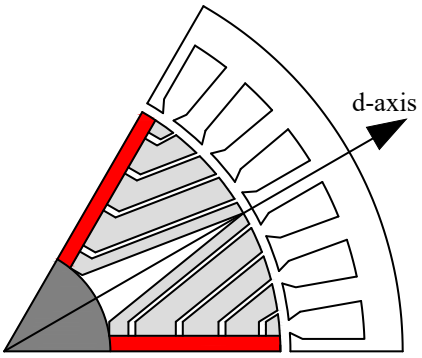

Figure 18. An NSPM machine with a segmented rotor design. Figure adapted from [105].

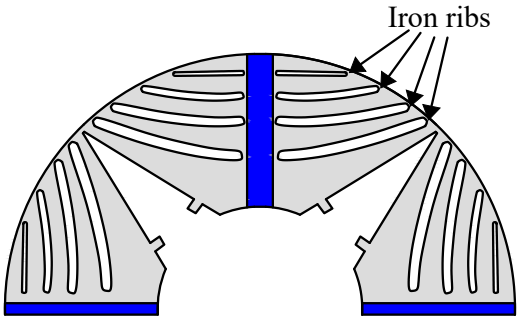

Figure 19. Iron ribs in the segmented rotor design of an NSPM machine. Figure adapted from [106].

In [107], the authors proposed a general theory to assess the impact of rotor segmentation on the electromagnetic performance of a PMSM. The authors studies the impact of two types on rotor segmentation: (1) along the d-axis and (2) along the q-axis, as shown in Figure 20a and Figure 20b, respectively. It is shown that for small values of the flux gap thickness, there is little impact on the average torque. Under certain design constraints, segmentation along the q-axis can lead to an increase in the reluctance torque. For applications demanding field-weakening operation, increased reluctance torque shows promising opportunities for design improvement.

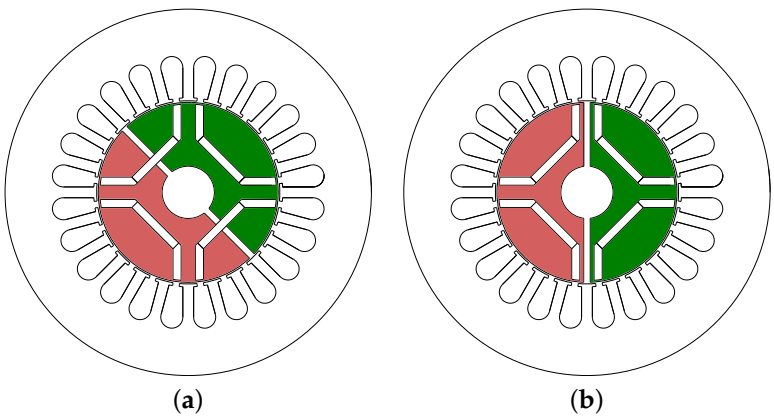

Figure 20. Segmented rotor PMSM designs [107]. (**a**) Segmentation along d-axis, (**b**) Segmentation along q-axis.

A conventional interior PM (IPM) rotor consists of thin steel bridges at the rotor outer surface, which are responsible for the mechanical retention of magnets. However, these bridges also provide a closing path for leakage flux. With the use of segmented rotor structure, these bridges can be removed, leading to an increase in the magnet flux linkage and, therefore, the torque density of the machine. This concept has been investigated by many authors [108–110], including the recent Tesla Model S Plaid motor [111]. However, the removal of retention bridges can lead to structural failure. Using additional retention sleeves like the ones used in a surface-mounted PM (SPM) rotor will increase the magnetic air gap length and contribute negatively to the torque production. In [108,109], nonmagnetic wedge materials were used to maintain the structural integrity, as shown in Figure 21. It is worth mentioning that optimizing the shape of the wedge also improved the electromagnetic performance of the machine. On the other hand, a self-locking design, which satisfies the structural requirements at 12,000 RPM, for a consequent pole PMSM was proposed in [110], as shown in Figure 22. A brief comparison of the segmented rotor designs used in SRMs and PMSMs is presented in Table 3.

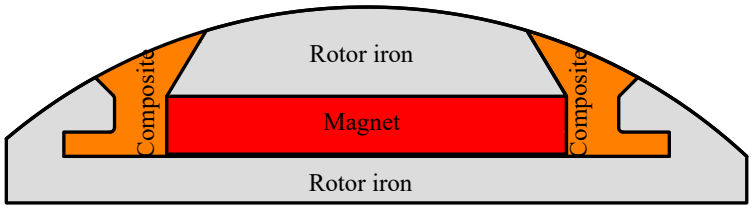

Figure 21. IPM rotor pole design with nonmagnetic wedge for magnet retention. Figure adapted from [109].

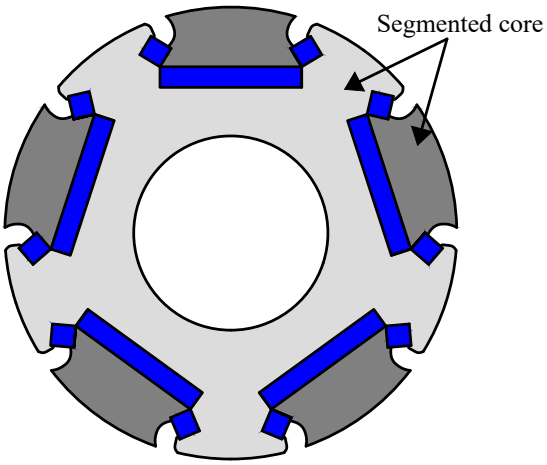

Figure 22. Novel modular rotor with self-locking design for retention of magnets. Figure adapted from [110].

Table 3. Comparison of segmented rotor designs used in SRMs and PMSMs.

Feature	Segmented Rotor SRM	Segmented Rotor PMSM
Advantages	Shortened magnetic flux path, increased average torque, robust and easy assembly	Better overload performance, increased torque by removing bridges, can increase reluctance torque
Limitations	High eddy current loss with aluminum hub design, high torque ripple	Complex rotor assembly, structural concerns without retention bridges
Suitability	SRMs designed for increased mechanical strength	PMSMs with better field-weakening performance

4. Core Loss of Segmented Cores

The magnetic properties of electrical steel lamination deteriorate close to cut edges. Microstructural changes due to cutting result in decreased magnetic permeability and increased core loss in the region close to the cut edge [46,112–114]. Maximum material degradation is observed at the cut edge, which gradually decreases as one moves farther away from it. While the maximum degradation of magnetic properties at the cut edge is a material constant, the maximum distance from the cut edge where the properties are degraded depends on the geometry of the lamination, sample grain size, cutting technique [115], and tool clearances [45,116]. In most cases, manufacturers use the standard Epstein frame test to determine the lamination's material properties. Naturally, the data include the impact of only two cut edges present in a steel sheet of a size according to international standards, such as IEC 60404-2 [117] and IEC 60404-10 [118]. It is shown in [119] that the core loss of a steel sheet increases as the number of segments and cut edges present in the sheet increase. Consequently, the material properties from the standard Epstein frame test cannot accurately calculate the core loss of a conventional stator geometry, where several cut edges are present in a lamination. The segmentation of stator introduces additional cut edges in an assembled lamination, which will further increase the core loss.

The current literature on analyzing the impacts of the cut edges can be classified into two categories: (1) cut edge characterization and (2) performance evaluation of machines with cut edge effect.

4.1. Cut Edge Characterization

Several methods have been explored to determine the dependence of the deteriorated magnetic properties on the distance from the cut edge. Since the magnetic properties of the material are affected by its mechanical state, most methods involve estimating the cut edge width by analyzing a mechanical parameter, such as the residual elastic stress or plastic strain profile in the affected region. Zero residual strain levels have been reported in the bulk material, which means it remains unaffected by the cut edge. Then, the electrical sheet specimen is characterized by having been pre-subjected to several strain levels. Consequently, a strain-dependent nonlinear BH model can be developed. However, the variation in elastic stress or plastic strain near the cut edge is highly nonlinear [120]. Consequently, determining an accurate spatial distribution of the desired mechanical state and, therefore, the magnetic properties is a difficult task.

Some methods to estimate the cut edge width include magnetic needle probe measurements [46], micro-Vickers hardness measurements [120–122], Kerr effect microscopy [123], electron backscatter diffraction (EBSD) [115,124], and a combination of nano-indentation and EBSD kernel average misorientation (KAM) maps [125]. It must be mentioned that the estimation accuracy is impacted by the method's resolution, and different values of the cut edge width ranging from 0.5 mm to several mm have been reported in the literature. In [45], a parabolic distribution function was used to define the dependence of magnetic properties on the distance from the cut edge. Experimental characterization is performed using rectangular sheet specimens with different numbers of segments, with the total width kept constant to 80 mm for each sheet. The method assumes that the maximum permeability drop ($\Delta\mu_{cut}(H)$), which happens at the cut edge, is a material constant. Then, in utilizing the global (averaged over an entire cross-section) measurements and the fact that the $\Delta\mu_{cut}(H)$ is independent of the number of segments, the spatial distribution of permeability in the cut edge width can be found.

In [126,127], a combination of experimental measurements and FEA is proposed to estimate the impact of cut edges. Two laminated toroidal cores of equal thickness are experimentally characterized: (1) unsegmented (undamaged) core and (2) segmented

(partially damaged) core made of five concentric rings. A 2D FEA model of the two tested rings is created. The partially damaged core is modeled using two types of homogeneous regions, undamaged and damaged, as shown in Figure 23. Since the maximum and minimum radii of each elementary ring are known, the cut edge width is changed until the FEA results match the globally measured flux density values. To match the values, the flux density is assumed to be nearly zero in the damaged zone when the global measurement is less than 0.8 T. In addition, an exponential magnetic permeability distribution from the cut edge is defined. Once the cut edge width is finalized, the magnetic properties for the damaged zone can be calculated. However, such a simple approximation of the damaged zone is unsuitable for all manufacturing methods. Even though one damaged zone may work for punching, three damaged zones with different properties are required for laser cutting, which increases the model complexity [127].

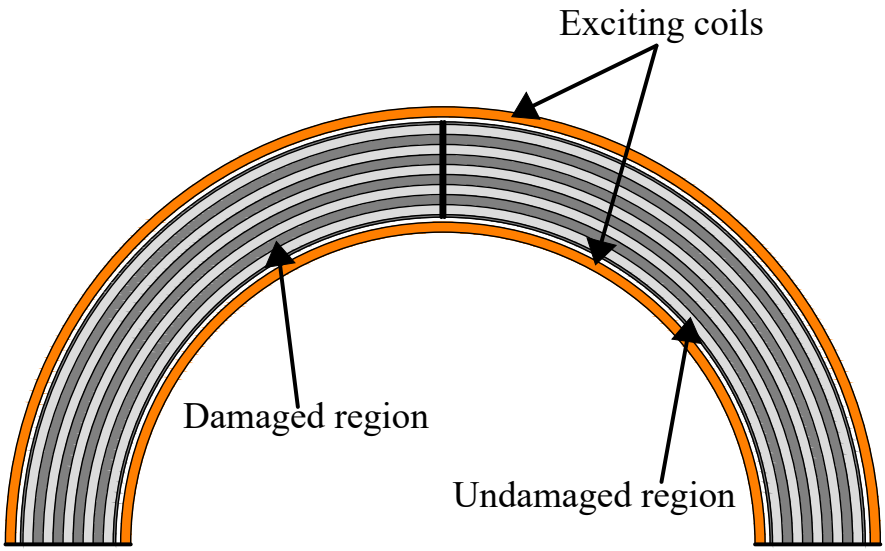

Figure 23. Two-dimensional FEA model of the tested, partially damaged toroidal core. Figure adapted from [126].

4.2. Performance Evaluation of Machines with Cut Edge Effect

The impact of cut edges on the core loss of an electrical machine has been investigated by many researchers. Most methods can be attributed to improving the FEA modeling of cut edges, which is essential to improving the machine design process. The magnetic properties determined from the cut edge characterization are utilized to calculate the magnetic flux density distribution and the core loss distribution in the electrical steel. Several FEA models have been proposed in the literature, ranging in complexity and accuracy.

4.2.1. Conventional Machines

A simple model was proposed in [128], where an inner zone close to the cut edge was modeled in the stator tooth and yoke geometry, as shown in Figure 24. Here, the inner zone defines a region with plastic deformation and is subjected to residual mechanical stress during simulations. The thickness of the deformed region is considered to be half the thickness of the steel sheet. In addition, stress-dependent BH curves are used to calculate the flux density distribution and the core loss of the stator. The proposed model was compared with the experimental results from the rotational loss measurement procedure described in [129]. While the presented FEA results show a deviation of about 10% from the experiments, the details of the operating point chosen for the analysis are not clear.

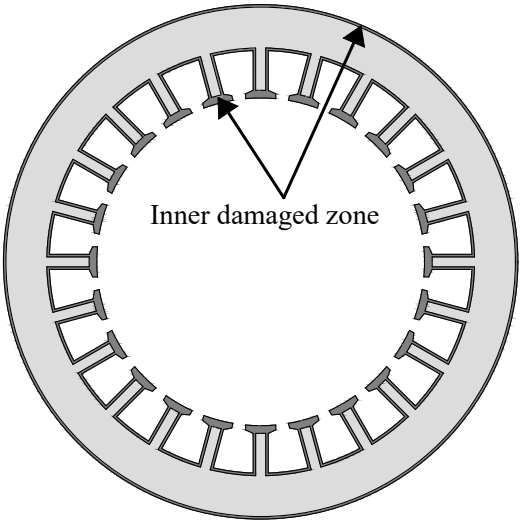

Figure 24. Two-dimensional FEA model with cut edge effect included. Figure adapted from [128].

A more accurate FEA model was proposed in [130], where a total of five zones are introduced in the stator and rotor FEA geometry, as shown in Figure 25. Each zone is assigned different magnetic properties based on the model proposed in [45]. Zone 5 is assumed to be free from any cut edge effect. It is worth noticing that the accuracy of such a model will increase as the number of modeled zones is increased. However, it will also increase the model complexity. Moreover, the selection of an appropriate number of zones is a challenging task and might require a few tries to reach the optimal number. A similar, but more general approach is presented in [131], where an exponential degradation function $\gamma(s) \in [0, 1]$ is used to model the magnetic properties in the affected region. The exponential profile is an approximation of the nonlinear BH model determined by the cut edge characterization. The approximated function is used to discretize the affected region in a sufficient number of layers, each with different magnetic properties. The stator core loss is calculated after processing the magnetic flux density distribution. The model's results were compared with the experimental results for two machines, showing promising results for one of the machines.

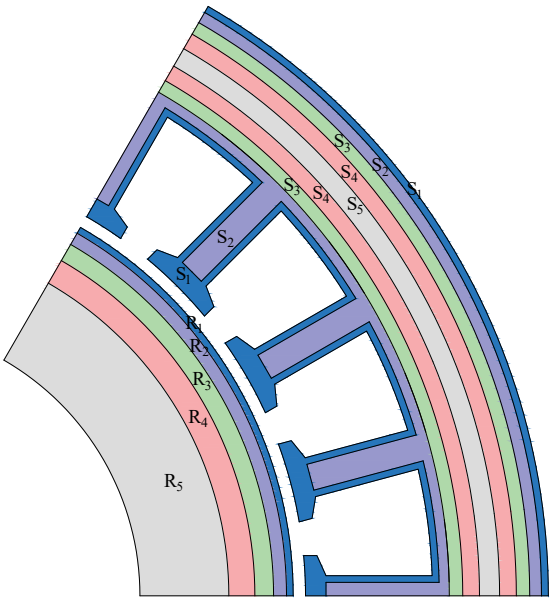

Figure 25. Five zones to model the cut edge effect in stator and rotor geometry. Figure adapted from [130].

The selection of an optimal number of discretized zones or layers is a difficult task. Moreover, each discrete zone is modeled with homogeneous magnetic properties, which does not reflect the true impact of the cutting process. Therefore, several researchers have explored a continuous modeling technique [116,132–134]. Here, a continuous BH model was used to show the negative impact of cut edges on the core loss of the stator of an electric machine. First, experimental investigations were performed with several cut edges on the electrical steel specimen. Then, a nonlinear BH model, such as the one described in [45], was determined to explain the impact of distance from the cut edge on the magnetic properties. With this knowledge, the magnetic properties in each mesh element of the FEA model can be defined based on its distance from the cut edge. Even though the proposed modeling technique is simpler with no added geometric complexity, the accuracy of the modeled fits decrease with an increase in number of cut edges as the selection of an appropriate distribution function becomes challenging.

4.2.2. Segmented Machines

The impact of cut edges on the core loss of a segmented machine design is a relatively understudied problem. An FEA model inspired from [130] is proposed to capture the impact of additional cut edges due to the segmentation in [29]. The proposed model was used to compare the core losses of two different segmented stator designs: (1) segmentation at the yoke and (2) segmentation at the root of each tooth, as shown in Figure 26a and Figure 26b, respectively. Analysis reveals that for the same operating point, the stator with segmentation at the yoke has lower core loss. The proposed model can be utilized to compare the core losses of two different segmented stator designs. Nevertheless, the complexity of the FEA model is increased significantly compared to that of a conventional design.

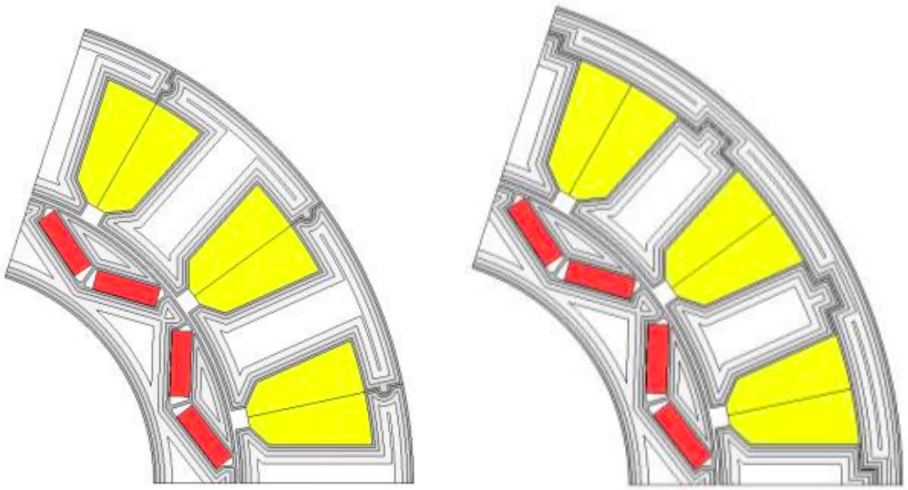

(**a**) (**b**)

Figure 26. Two-dimensional FEA model with cut edge effect included [29]. (**a**) Segmentation at the yoke. (**b**) Segmentation at the root of each tooth.

The modeling approaches presented in [132–134] can also be applied to analyze the core loss of a segmented stator. However, such modeling techniques are rather complex and cannot capture the true impact of the segmentation anyway. Segmentation not only introduces additional cut edges, but parasitic gaps and additional stress developed due to the assembly process, all of which impact the core loss of an assembled core. The modeling of such physical phenomena considering manufacturing uncertainties is an extremely difficult task. Consequently, experimental investigations using manufactured stators are required, which are scarce and scant in providing enough insight to electric machine engineers.

A single-tooth tester (STT) measurement system for the magnetic characterization of a stator segments made of a soft magnetic composite (SMC) was proposed in [135,136]. The experimental setup consists of two measurement yokes with excitation and measurement coils, as shown in Figure 27. Since the recorded measurements are the sum of the core loss of the stator tooth segment and the two measurement yokes, a loss separation approach is proposed. A digital twin of the test bench was created in FEA. For each operating point, the loss in the tooth segment was estimated by modifying the Bertotti loss coefficients so that the simulation results matched the measured values. While the proposed method is useful in assessing the impact of manufacturing conditions and application of different materials on the core loss of a single tooth, it does not provide insight about the core loss distribution in the tooth and back iron region of the segment.

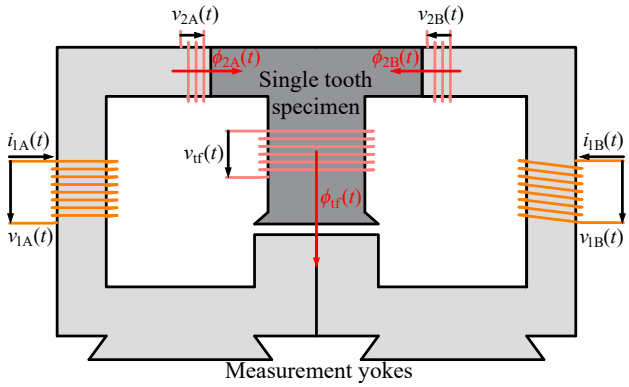

Figure 27. Schematic model of the single-tooth test (STT) bench. Figure adapted from [135].

An experimental technique to separate the core loss in a stator segment's tooth and back iron region is presented in [137]. Here, the experimental setup consists of a manufactured segmented stator, an H-shaped device made of electrical steel laminations (H-Sensor), a drive coil to impose the excitation current, a pickup coil to measure the induced voltage, and a control coil to ensure the sinusoidal injection of magnetic flux in the stator teeth, as shown in Figure 28. With the use of lumped parameter theory, the active part of the segmented stator is divided into three isotropic segments: T, T′, and X. Consequently, the core loss of the segmented stator section is the sum of the individual core loss of the three segments. To solve these three unknowns, three H-Sensors spanning different numbers of stator teeth were utilized. Experimental measurements were used to demonstrate the negative impact of segmentation on core loss. The separation of core loss in the tooth and back iron region can benefit the line testing of the manufactured stators. Increased core loss in a specific region can help identify the defective tool quickly, leading to decreased downtime. Understanding how segmentation impacts core loss in specific regions can lead to more efficient use of low-loss materials such as oriented steel in electric machine designs. Different advantages and limitations related to FEA modeling and experimental evaluation techniques are summarized in Table 4.

Table 4. Comparison of FEA modeling and experimental evaluation techniques for estimating core loss performance of segmented stators.

Feature	FEA Modeling	Experimental Evaluation
Advantages	Quick estimation of core loss, flexibility to analyze different designs, useful for comparative studies	Accurate measurement of core loss, includes impact of assembly process, beneficial for line testing
Limitations	Selection of appropriate discrete zones, practical implementation	Availability of manufactured stators

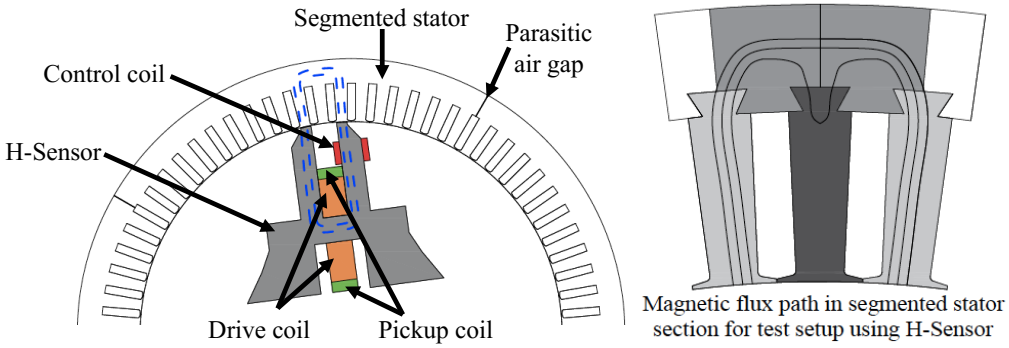

Figure 28. Experimental setup used for separation of core loss in tooth and back iron region of segmented stator. Figures adapted from [137].

5. Application of Oriented Steel in Construction of Segmented Cores

A segmented stator or rotor design can lead to inferior machine performance due to unavoidable parasitic gaps and additional cut edges. The utilization of oriented steel can help mitigate these detrimental impacts on electromagnetic performance and core losses. Grain-oriented electrical steel (GOES), also known as anisotropic steel, features a unique crystal structure where the grains are aligned predominantly in the rolling direction (0°). Consequently, GOES exhibits significantly superior magnetic performance to non-grain-oriented electrical steel (NGOES) when the magnetic field aligns with the rolling direction. However, the magnetic properties of GOES deteriorate as the direction of the magnetic flux changes, with the worst properties seen at 55° [51,75,138], as shown in Figure 29.

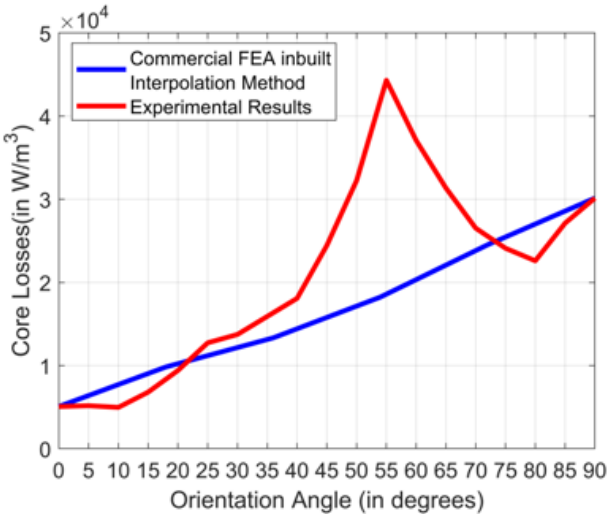

Figure 29. Variation in core loss with orientation angle obtained from experimental results. Figure adapted from [75].

It is also reported that the properties of NGOES are almost similar to the GOES properties in the transverse direction. Consequently, the use of oriented steel in a non-segmented design is limited, where every second lamination in the stack must be shifted by an optimal spatial angle [139–141]. Oriented steel is predominantly employed with segmented lamination in AC electric machines to increase the extent of potential benefits observed in the performance.

5.1. Performance Improvement with Oriented Steel

The performance of a segmented SRM is improved by employing GOES in the rotor of a six-slot/four-pole machine [142]. Authors have proposed two types of rotor construction

with oriented steel, as shown in Figure 30a and Figure 30b, respectively. The performances of the two proposed designs are compared with the conventional NGOES design using analytical and experimental methods. Analytical results indicate improved machine performance with GOES designs regardless of the operating speed. On the contrary, experimental results show that while GOES designs improve the motor efficiency by 1.5% at 1800 RPM, there is no significant change in the performance at 600 RPM. The two methods' different results highlight a nonlinear relationship between the operating frequency and the impact of the cut edges on core loss, which is not accounted for in the analytical calculations.

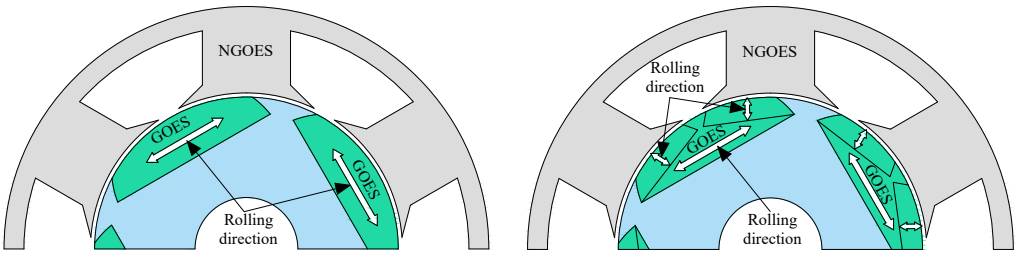

Figure 30. Segmented rotor designs manufactured using oriented steel for a six-slot/four-pole SRM. Figures adapted from [142].

The direction of magnetic flux in the stator teeth of a radial flux machine is mostly radial. Changing the material in stator teeth from NGOES to GOES can improve the motor performance, if the rolling direction is maintained in the direction of the arrows, as shown in Figure 31. This concept is utilized to improve the performance of a 48-slot motor in [143]. Experimental results from the manufactured prototype show that even with a 48-segmented-teeth construction, the motor output torque and efficiency increase with the introduction of GOES in stator teeth. Notably, the reported relative increase in motor efficiency is higher at higher speeds. In axial flux PM (AFPM) machines, the magnetic flux flow in the stator tooth is uni-directional (axial). Thus, yoke-less AFPM stator cores can be constructed using segmented GOES sheet lamination, which provides better magnetic properties compared to NGOES material and can improve the motor performance [144,145].

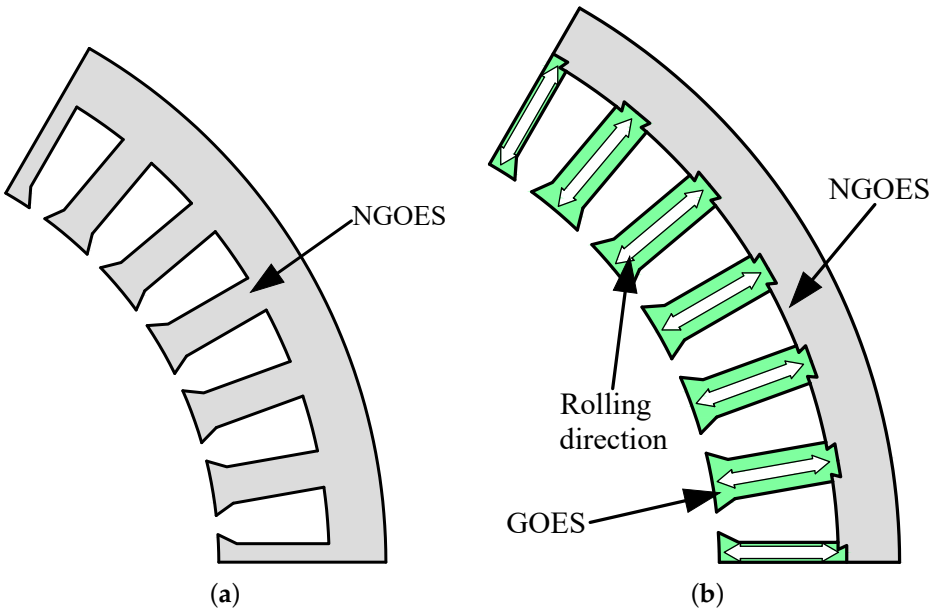

Figure 31. An electric machine stator with (**a**) NGOES teeth and (**b**) GOES teeth. Figures adapted from [143].

A segmented rotor constructed using oriented steel for the electromagnetic performance improvement of a four-pole SynRM was proposed in [146]. To improve the structural integrity of the assembled rotor, irregular thickness at the segment edges $d1$ and $d2$ is proposed, as shown in Figure 32. This way, a zig-zag pattern can be created by flipping the segments in every alternate layer, which is further strengthened by applying a bonding adhesive. The q-axis of each individual pole segment is perpendicular to the rolling direction, which enhances the magnetic properties in ribs, as the direction of magnetic flux is almost parallel to the rolling direction. A segmented design improves the saliency ratio as the magnetic properties along the d-xis are superior to those along the q-axis. Moreover, the two edges of a barrier, $e1$ and $e2$, are placed such that torque pulsations generated from the interaction of stator slots with both edges cancel each other out. Thus, torque ripple is decreased, and average torque can be increased.

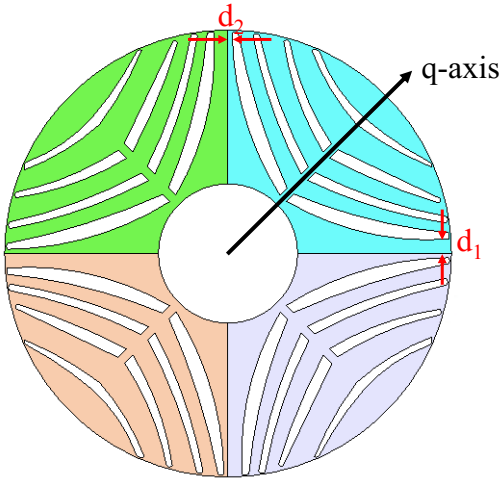

Figure 32. Segmented rotor design used in a four-pole SynRM. Figure adapted from [146].

A new segmented stator design for FSCW PMSM using GOES is presented in [147]. Here, GOES sheet strips are bent to create a horseshoe-shaped segmented stator core, as shown in Figure 33. Since the bending of lamination imposes added manufacturing limitations, the GOES design has open stator slots, and the stator yoke thickness is half of tooth width. Consequently, the flux density in stator yoke is increased but decreased in stator teeth. In keeping the physical dimensions of the motor constant, the stator core with GOES material decreases torque ripple, increases average torque, and decreases the core loss of the machine. However, the presented conclusions are based on the FEA results of the machines, which only include the impact of parasitic gaps on the motor performance.

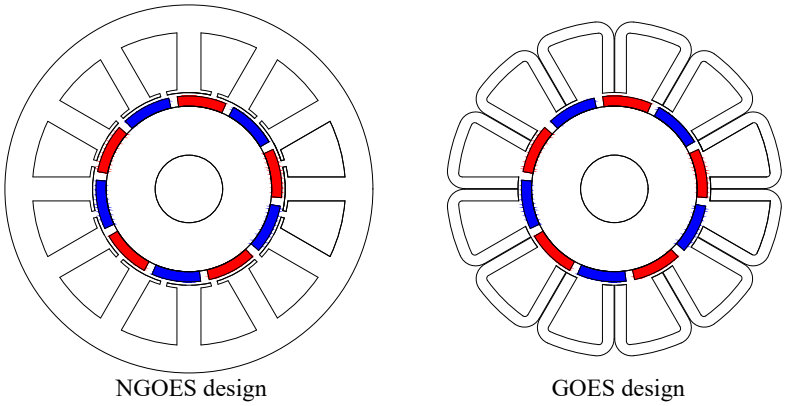

Figure 33. New segmented stator topology with GOES for 12-slot/10-pole FSCW PMSM. Figures adapted from [147].

5.2. FEA Modeling of Segmented Stators Constructed Using Oriented Steel

Recent advancements in finite-element analysis (FEA) software have significantly improved the ability to estimate key performance parameters of electric machines with reasonable accuracy. By enabling performance prediction prior to manufacturing, FEA helps identify potential design challenges early and provides an intuitive platform for resolving them. Effectively utilizing oriented steel in the construction of segmented stators requires that machine designers employ appropriate and accurate modeling techniques. However, the magnetic properties of GOES are highly dependent on the direction of the magnetic flux and exhibit a behavior that is neither linear nor elliptical [148]. The magnetic permeability of anisotropic materials is highest in the rolling direction (0°), lower in the transverse direction (90° relative to the rolling direction), and lowest at angles around 50°–60° from the rolling direction. In contemporary finite-element analysis (FEA) software, the magnetic properties, B-H curves, and loss curves of the rolling and transverse directions are used to interpolate the magnetic properties for intermediate directions. However, this interpolation method is not user-controlled, which can lead to inaccuracies in the simulation results. Moreover, it is unclear if the specific variations in magnetic properties with change in the flux direction can be generalized to all anisotropic steel materials. Consequently, the FEA modeling of oriented steel is a challenging task.

To address these challenges, researchers and engineers have explored advanced modeling techniques and more sophisticated interpolation methods. These efforts aim to improve the accuracy of simulations by better capturing the complex magnetic behavior of anisotropic materials. Enhanced modeling approaches could include the development of user-defined interpolation functions, the incorporation of more detailed material characterization data, and the use of machine learning algorithms to predict magnetic properties more accurately. By refining these techniques, it is hoped that the reliability and precision of FE simulations involving anisotropic materials will be significantly improved, leading to better performance predictions and optimized designs.

An accurate but cumbersome way to model the oriented steel in FEA is to use multiple BH curves extracted at different orientation angles, as suggested in [149]. One way to avoid working with multiple BH curves is to use more complex models, such as the E&S model suggested by Enokizono and Soda [150,151]. The vector magneto-hysteretic E&S model utilizes the concept of two-dimensional magnetic properties and experimental measurements to calculate the distribution of locus for B and H vectors. It is shown that the relationship between the B and H vectors is dependent on the level of magnetic induction, the axis ratio of rotating flux α ($=B_{min}/B_{max}$), and the angle of inclination against the easy (rolling) axis direction ϕ, as shown in Figure 34. Another model is suggested in [50], where the anisotropy is modeled with the help of equivalent magnetic field components calculated using magnetic co-energy densities in the three principal directions for a given magnetic field. Such complex modeling techniques can improve the accuracy of results at the expense of simplicity [50,149–153].

In [28], a method was developed for finite-element analysis (FEA) to accurately evaluate the performance of permanent magnet synchronous motors (PMSMs) with GOES stator laminations. This method involves dividing the stator into sections and assigning BH curves and loss curves to each section based on the direction of flux flow. Consequently, the simulation is simplified to a connected structure of isotropic materials. Due to this structure, the proposed model is referred to as a piecewise isotropic model in this study. The machine analyzed in [28] is a 12-slot/14-pole PMSM composed of six segments, with each segment oriented in the direction of the teeth.

The direction of orientation of one segment and the direction of flux flow in the entire machine as well as within a segment under no-load conditions are illustrated in Figure 35.

In one segment, the flux flow direction for the middle tooth aligns with the rolling direction (i.e., 0°), while for the adjacent two teeth, it deviates by 30° from the rolling direction. The flux direction in the back iron between the middle tooth and the adjacent tooth shifts from 90° to 60°. The model proposed in [28] connects the segments using the BH and loss curves for the 0° direction on the central tooth, the 30° direction on the lateral teeth, and the 75° direction for the back iron, which is the average of 60° and 90°. Figure 36 presents the model of one segment, and the complete machine is modeled by connecting six segments circumferentially.

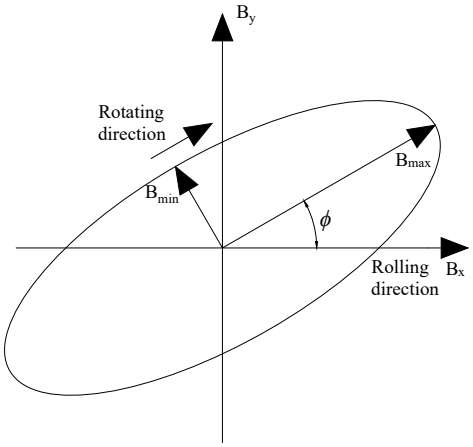

Figure 34. Relationship between maximum flux density B_{max}, axis ratio α, and inclination angle ϕ. Figure adapted from [150].

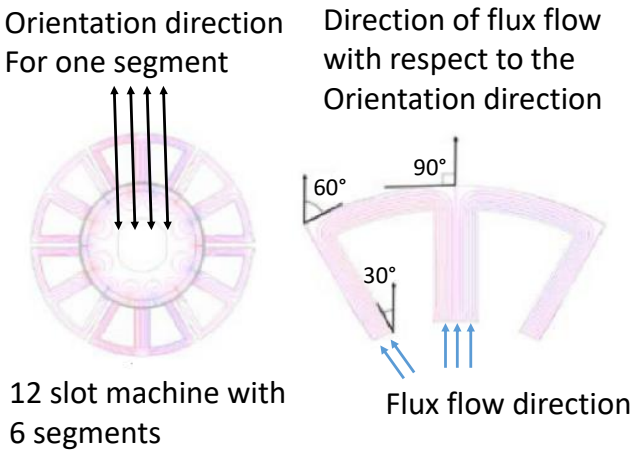

Figure 35. Direction of orientation and flux flow direction in the whole machine and one segment under no-load condition [28].

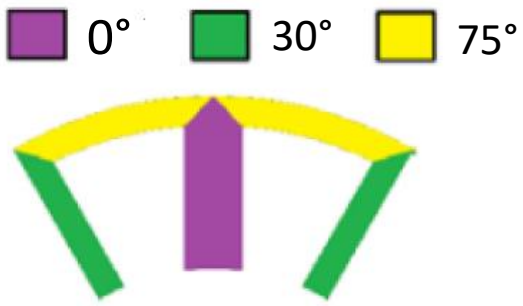

Figure 36. Piecewise isotropic model used for analysis, with each color representing a different angle away from the rolling direction. These colors correspond to the magnetic properties of the oriented steel at those specific angles [28].

The piecewise isotropic model, illustrated in Figure 36, can accurately model a PMSM if the magnetic properties, such as BH and loss curves, of the steel are known at specific angles relative to the rolling direction. These angles are determined by the relative positions of adjacent teeth and the orientation direction of the GOES material. Similar FEA modeling approaches were utilized in [75,154]. While the model leverages the distinct distribution of magnetic properties along the principal axes, it assumes that the isotropic properties are equivalent to the average flux direction. This rough approximation of magnetic properties can result in inaccurate predictions of motor performance, especially in machines with a low number of slots.

A more accurate isotropic modeling technique was proposed in [155]. The proposed model divides a GOES stator segment into three isotropic parts: (1) stator tooth, (2) back iron behind the stator slot, and (3) back iron behind the stator tooth. The division of the back iron section into two different isotropic segments stems from the fact that the direction of flux flow in the back iron region behind the slot is always in the circumferential direction, whereas, the direction of flux flow in the back iron region behind the stator tooth changes in one electrical cycle and is a combination of the four cases, as shown in Figure 37.

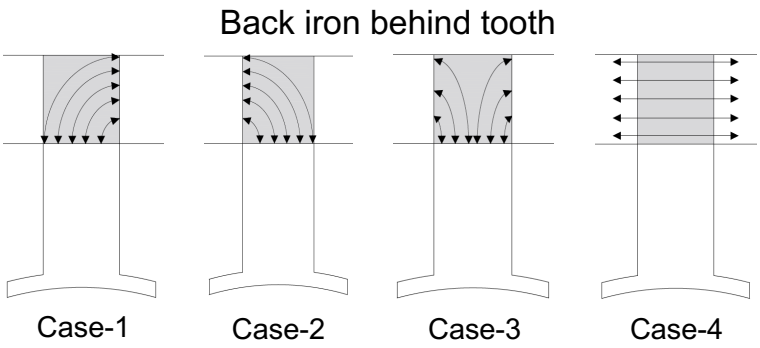

Figure 37. Four cases showing changing direction of magnetic flux in back iron behind stator tooth in one electrical cycle. Figure adapted from [155].

A mathematical technique is presented to determine the magnetic properties of all isotropic sections based on the direction of magnetic flux. Authors have shown that the magnetic properties in the back iron region behind the slot correspond to the average of the magnetic properties of the direction of flux and not the average of the directions, as shown in Figure 38. Moreover, the properties in the back iron region behind the stator tooth are more complex and are derived using the direction of magnetic flux of four cases. Designers should note that the accuracy of the model depends on the precision of the available (measured) magnetic properties in different directions. A brief summary of different GOES modeling techniques is presented in Table 5.

Table 5. Comparison of techniques used for FEA modeling of oriented steel.

Modeling Technique	Advantages	Limitations
Multiple BH Curves	High accuracy and precision	Requires significant experimental data
E&S Model	Captures two-dimensional behavior accurately	Complex implementation, non-standard experimental setup
Piecewise Isotropic Modeling [28]	Simplified Modeling, fast computation	Crude approximation of direction of flux, inaccurate for a low number of slots
Piecewise Isotropic Modeling [155]	Improved accuracy in modeling back iron region	Complex modeling of back iron region behind stator tooth

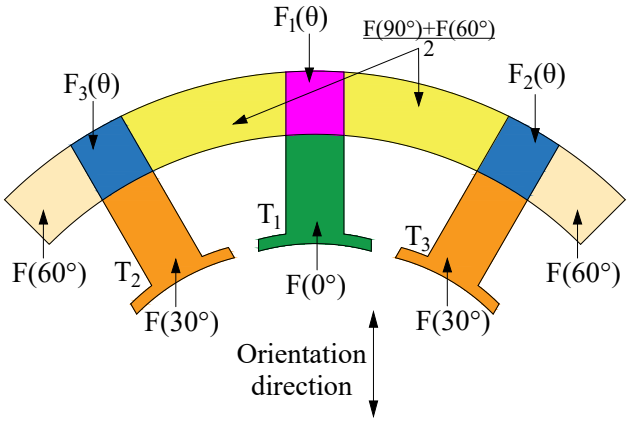

Figure 38. Equivalent piecewise isotropic model for one segment, with each color representing a different angle away from the rolling direction. The model consists of three isotropic segments: (1) stator tooth, (2) back iron behind stator slot, and (3) back iron behind stator tooth. Figure adapted from [155].

6. Conclusions

This paper provides a comprehensive review of segmented stators and rotors in electric machines. The discussion begins with an exploration of various manufacturing techniques for segmented stator and rotor cores, highlighting the unique advantages and challenges associated with each method. This is followed by an analysis of how common stator and rotor segmentation designs affect the electromagnetic performance of AC electric machines, presenting both the benefits and limitations of such designs. Depending on the segmentation technique, the magnetic flux linkage and average torque can be increased or decreased by carefully managing the parasitic gaps between segments. Furthermore, this paper examines the impact of additional cut edges on core loss, a consequence inherent to segmented stator designs. Methods for characterizing cut edge width and approaches to model the effects of cut edges in core loss estimation are thoroughly discussed. While numerical modeling is effective for comparative analyses between designs, the accurate measurement of core loss still requires experimental validation, which can also help the line testing of manufactured segmented stators. Additionally, this paper investigates the use of oriented steel for improving the performance of AC electric machines. Since capturing material anisotropy remains challenging, this paper also delves into the complexities of the finite-element analysis (FEA) modeling of anisotropic steel within segmented stator designs.

Overall, this review serves as a valuable resource for machine designers by providing critical insights into the application, design, and performance enhancement of electric machines employing segmented stators and rotors. These insights can be leveraged to achieve accurate modeling, optimize performance, or expand the existing knowledge base in this field.

Despite substantial progress in segmented stator and rotor designs, critical knowledge gaps continue to hinder further advancements. While the current literature has made significant strides in modeling cut edge effects, the FEA modeling of oriented steel, and evaluating the impact of individual stator and rotor segmentation on machine performance, several key questions remain unanswered. Addressing these gaps is essential for advancing understanding and developing more accurate and robust performance evaluation models for such machines.

Referring to Figure 20, the discussion highlights how rotor segmentation can enhance reluctance torque by increasing the saliency ratio compared to conventional machines. Combining segmented rotor designs with segmented stator constructions could offer the potential to further increase the saliency ratio, offsetting any reduction in magnetic torque

and improving overall performance, specifically in the field-weakening region. However, analyses investigating the combined effects of segmented stators and rotors are notably absent in the current literature.

In Figure 26, the focus shifts to cut edge modeling in numerical analysis, emphasizing the physical effects of increased stamping impacts in segmented stator designs. While the proposed method demonstrates high accuracy, its practical implementation remains a significant challenge. Therefore, there is a need for a simpler and precise method to incorporate the impact of cut edges on the performance of segmented stator machines. The proposed division of core losses, as shown in Figure 28, between individual teeth and back iron delivers promising results by effectively capturing the influence of orientation and increased cut edges caused by segmentation. However, a deeper investigation is required, particularly using stators where the back iron and teeth are oriented in different directions, to fully understand the effects of increased cut edges under varying orientation conditions.

Figure 38 presents an improved FEA model for oriented steel segmented stators, employing a piecewise isotropic approach based on the direction of orientation and magnetic flux. While this approach shows promise, its applicability could be further enhanced by developing generalized expressions for defining the anisotropic magnetic properties of isotropic segments. Such generalization should account for the precision of known magnetic properties and stator design parameters, highlighting any loss of accuracy when the precision is insufficiently refined.

Author Contributions: Conceptualization, B.K.; methodology, B.K. and A.A.; software, B.K., A.A. and S.F.; validation, B.K., A.A. and S.F.; formal analysis, B.K., A.A. and S.F.; investigation, B.K., A.A. and S.F.; resources, B.K., A.A. and S.F.; data curation, B.K., A.A. and S.F.; writing—original draft preparation, B.K.; writing—review and editing, B.K., A.A. and S.F.; visualization, B.K., A.A. and S.F.; supervision, S.F.; project administration, S.F.; funding acquisition, S.F. All authors have read and agreed to the published version of the manuscript

Funding: This research received no external funding.

Conflicts of Interest: The authors declare no conflicts of interest.

References

1. Electrical and Electronics Technical Team Roadmap. Available online: https://www.energy.gov/sites/prod/files/2017/11/f39/EETT%20Roadmap%2010-27-17.pdf (accessed on 1 July 2024).
2. Commission Regulation (EU). *Commission Regulation (EU) 2019/1781 of 1 October 2019 Laying Down Ecodesign Requirements for Electric Motors and Variable Speed Drives Pursuant to Directive 2009/125/EC of the European Parliament and of the Council, Amending Regulation (EC) No 641/2009 with Regard to Ecodesign Requirements for Glandless Standalone Circulators and Glandless Circulators Integrated in Products and Repealing Commission Regulation (EC) No 640/2009 (Text with EEA Relevance)*; Commission Regulation (EU): Brussels, Belgium, 2019. Available online: http://data.europa.eu/eli/reg/2019/1781/oj (accessed on 1 July 2024).
3. Ionel, D.M.; Popescu, M. Finite-Element Surrogate Model for Electric Machines with Revolving Field—Application to IPM Motors. *IEEE Trans. Ind. Appl.* **2010**, *46*, 2424–2433. [CrossRef]
4. Alshaabani, A. Balanced Design of Three-Phase Coupled inductor. In Proceedings of the 2023 3rd International Conference on Electrical, Computer, Communications and Mechatronics Engineering (ICECCME), Tenerife, Canary Islands, Spain, 19–21 July 2023; pp. 1–4.
5. Islam, M.Z.; Bonthu, S.S.R.; Choi, S. Obtaining optimized designs of multi-phase PMa-SynRM using lumped parameter model based optimizer. In Proceedings of the 2015 IEEE International Electric Machines & Drives Conference (IEMDC), Coeur d'Alene, ID, USA, 10–13 May 2015; pp. 1722–1728.
6. Alshaabani, A.; Wang, B. Parasitic Capacitance Cancellation Technique by Using Mutual Inductance and Magnetic Coupling. In Proceedings of the IECON 2019—45th Annual Conference of the IEEE Industrial Electronics Society, Lisbon, Portugal, 14–17 October 2019; pp. 1928–1931.
7. Alshaabani, A.; Wang, B. Overall Parameters Affecting the Parasitic Capacitance of the Magnetic Components. In Proceedings of the 2022 IEEE 1st Industrial Electronics Society Annual On-Line Conference (ONCON), kharagpur, India, 9–11 December 2022 ; pp. 1–6.

8. Khoshoo, B.; Blank, J.; Pham, T.Q.; Deb, K.; Foster, S.N. Optimal design of electric machine with efficient handling of constraints and surrogate assistance. *Eng. Optim.* **2024**, *56*, 274–292. [CrossRef]
9. Huang, S.; Aggarwal, A.; Strangas, E.G.; Khoshoo, B.; Li, K.; Niu, F. Mitigation of Interturn Short-Circuits in IPMSM by Using MTPCC Control Adaptive to Fault Severity. *IEEE Trans. Power Electron.* **2022**, *37*, 4685–4696. [CrossRef]
10. Huang, S.; Aggarwal, A.; Strangas, E.G.; Li, K.; Niu, F.; Huang, X. Robust Stator Winding Fault Detection in PMSMs with Respect to Current Controller Bandwidth. *IEEE Trans. Power Electron.* **2021**, *36*, 5032–5042. [CrossRef]
11. Huang, S.; Strangas, E.G.; Aggarwal, A.; Li, K.; Niu, F. Robust Inter-turn Short-circuit Detection in PMSMs with Respect to Current Controller Bandwidth. In Proceedings of the 2019 IEEE Energy Conversion Congress and Exposition (ECCE), Baltimore, MD, USA, 29 September–3 October 2019; pp. 3897–3904.
12. Huang, S.; Bi, Z.; Sun, Z.; Aggarwal, A.; Huang, X.; Wu, L.; Niu, F. Detection of stator winding faults in PMSMs based on second harmonics of phase instantaneous reactive powers. *Energies* **2022**, *15*, 3248. [CrossRef]
13. Niu, F.; Zhang, P.; Zhou, F.; Huang, S.; Xu, Z.; Zhang, L.; Aggarwal, A. A Novel Method for Monitoring Stator Interturn Insulation Degradation of Inverter-Fed Motors Based on Impedance Spectrum Division. *IEEE Trans. Ind. Electron.* **2024**, 1–13. [CrossRef]
14. Niu, F.; Xu, M.; Zhou, F.; Huang, S.; Xu, Z.; Zhang, L.; Aggarwal, A. Accurate Interturn Short-Circuit Faults Diagnosis in PMSMs Under Variable Operating Conditions by Signal Compensation. *IEEE Trans. Power Electron.* **2025**, *40*, 3530–3542. [CrossRef]
15. Zhu, Z.Q.; Li, Y.X. Modularity techniques in high performance permanent magnet machines and applications. *CES Trans. Electr. Mach. Syst.* **2018**, *2*, 93–103. [CrossRef]
16. Lorenz, F.; Werner, R.; Paul, D.; Stein, T. Circumferentially Segmented Rotor Architecture for PMSM Traction Machines. In Proceedings of the 2020 International Conference on Electrical Machines (ICEM), Gothenburg, Sweden, 23–26 August 2020; pp. 2260–2265.
17. Albrecht, T.; Gürsel, C.; Lamprecht, E.; Klier, T. Joining techniques of the rotor segmentation of PM-synchronous machines for Hybrid drives. In Proceedings of the 2012 2nd International Electric Drives Production Conference (EDPC), Nuremberg, Germany, 15–18 October 2012; pp. 1–8.
18. Libert, F.; Soulard, J. Manufacturing Methods of Stator Cores with Concentrated Windings. In Proceedings of the 2006 3rd IET International Conference on Power Electronics, Machines and Drives - PEMD 2006, Dublin, Ireland, 4–6 April 2006; pp. 676–680.
19. Fitzgerald, A.; Kingsley, C.; Umans, S. *Electric Machinery*; McGraw-Hill International Edition; McGraw-Hill: New York, NY, USA, 2003.
20. Spooner, E.; Williamson, A. Modular, permanent-magnet wind-turbine generators. In Proceedings of the IAS '96. Conference Record of the 1996 IEEE Industry Applications Conference Thirty-First IAS Annual Meeting, San Diego, CA, USA, 6–10 October 1996; Volume 1, pp. 497–502.
21. EL-Refaie, A.M. Fractional-Slot Concentrated-Windings Synchronous Permanent Magnet Machines: Opportunities and Challenges. *IEEE Trans. Ind. Electron.* **2010**, *57*, 107–121. [CrossRef]
22. Akita, H.; Nakahara, Y.; Miyake, N.; Oikawa, T. New core structure and manufacturing method for high efficiency of permanent magnet motors. In Proceedings of the 38th IAS Annual Meeting on Conference Record of the Industry Applications Conference, Salt Lake City, UT, USA, 12–16 October 2003; Volume 1, pp. 367–372.
23. Chin, J.W.; Cha, K.S.; Park, M.R.; Park, S.H.; Lee, E.C.; Lim, M.S. High Efficiency PMSM with High Slot Fill Factor Coil for Heavy-Duty EV Traction Considering AC Resistance. *IEEE Trans. Energy Convers.* **2021**, *36*, 883–894. [CrossRef]
24. Dajaku, G. Elektrische Maschine. German Patent 102012103677 A1, 31 October 2013.
25. Dajaku, G. Electric Machine with a Stator Having Slots at the Tooth for Reducing the Fundamental Wave of the Magnetic Flux. U.S. Patent 10720801 B2, 21 July 2020.
26. Tata Steel. Available online: https://www.tatasteeleurope.com/automotive/products/electrical-steel (accessed on 1 July 2024).
27. Donaldson, P. Motor Laminations. Available online: https://www.emobility-engineering.com/motor-laminations/ (accessed on 1 July 2024).
28. Maraví-Nieto, J.; Azar, Z.; Thomas, A.S.; Zhu, Z.Q. Utilisation of grain-oriented electrical steel in permanent magnet fractional-slot modular machines. *J. Eng.* **2019**, *2019*, 3682–3686. [CrossRef]
29. Rens, J.; Jacobs, S.; Vandenbossche, L.; Attrazic, E. Effect of Stator Segmentation and Manufacturing Degradation on the Performance of IPM Machines, Using iCARe® Electrical Steels. *World Electr. Veh. J.* **2016**, *8*, 450–460. [CrossRef]
30. Tomida, T.; Sano, N.; Hinotani, S.; Fujiwara, K.; Kotera, H.; Nishiyama, N.; Ikkai, Y. Application of fine-grained doubly oriented electrical steel to IPM synchronous motor. *IEEE Trans. Magn.* **2005**, *41*, 4063–4065. [CrossRef]
31. Aggarwal, A.; Strangas, E. Review of Detection Methods of Static Eccentricity for Interior Permanent Magnet Synchronous Machine. *Energies* **2019**, *12*, 4105. [CrossRef]
32. Aggarwal, A.; Strangas, E.G.; Agapiou, J. Comparative Study of Offline Detection Methods of Static Eccentricity for Interior Permanent Magnet Synchronous Machine. In Proceedings of the 2019 IEEE 12th International Symposium on Diagnostics for Electrical Machines, Power Electronics and Drives (SDEMPED), Toulouse, France, 27–30 August 2019; pp. 75–81.

33. Aggarwal, A.; Allafi, I.M.; Strangas, E.G.; Agapiou, J.S. Off-Line Detection of Static Eccentricity of PMSM Robust to Machine Operating Temperature and Rotor Position Misalignment Using Incremental Inductance Approach. *IEEE Trans. Transp. Electrif.* **2021**, *7*, 161–169. [CrossRef]
34. Aggarwal, A.; Strangas, E.G.; Agapiou, J. Analysis of Unbalanced Magnetic Pull in PMSM Due to Static Eccentricity. In Proceedings of the 2019 IEEE Energy Conversion Congress and Exposition (ECCE), Baltimore, MD, USA, 29 September–3 October 2019; pp. 4507–4514.
35. Aggarwal, A.; Strangas, E.G.; Agapiou, J. Robust Voltage based Technique for Automatic Off-Line Detection of Static Eccentricity of PMSM. In Proceedings of the 2019 IEEE International Electric Machines & Drives Conference (IEMDC), San Diego, CA, USA, 12–15 May 2019; pp. 351–358.
36. Cao, W.; Mecrow, B.C.; Atkinson, G.J.; Bennett, J.W.; Atkinson, D.J. Overview of Electric Motor Technologies Used for More Electric Aircraft (MEA). *IEEE Trans. Ind. Electron.* **2012**, *59*, 3523–3531.
37. Szabo, L.; Ruba, M. Segmental Stator Switched Reluctance Machine for Safety-Critical Applications. *IEEE Trans. Ind. Appl.* **2012**, *48*, 2223–2229. [CrossRef]
38. Sui, Y.; Yin, Z.; Cheng, L.; Zheng, P.; Tang, D.; Chen, C.; Wang, C. Multiphase Modular Fault-Tolerant Permanent-Magnet Machine with Hybrid Single/Double-Layer Fractional-Slot Concentrated Winding. *IEEE Trans. Magn.* **2019**, *55*, 1–6. [CrossRef]
39. Li, G.J.; Ren, B.; Zhu, Z.Q.; Foster, M.P.; Stone, D.A. Demagnetization Withstand Capability Enhancement of Surface Mounted PM Machines Using Stator Modularity. *IEEE Trans. Ind. Appl.* **2018**, *54*, 1302–1311. [CrossRef]
40. Li, G.J.; Zhu, Z.Q.; Foster, M.P.; Stone, D.A.; Zhan, H.L. Modular Permanent-Magnet Machines with Alternate Teeth Having Tooth Tips. *IEEE Trans. Ind. Electron.* **2015**, *62*, 6120–6130. [CrossRef]
41. Zhu, Z.Q.; Azar, Z.; Ombach, G. Influence of Additional Air Gaps Between Stator Segments on Cogging Torque of Permanent-Magnet Machines Having Modular Stators. *IEEE Trans. Magn.* **2012**, *48*, 2049–2055. [CrossRef]
42. Li, G.J.; Zhu, Z.Q.; Chu, W.Q.; Foster, M.P.; Stone, D.A. Influence of Flux Gaps on Electromagnetic Performance of Novel Modular PM Machines. *IEEE Trans. Energy Convers.* **2014**, *29*, 716–726. [CrossRef]
43. Li, G.J.; Liang, X.B.; Zhu, Z.Q.; Ojeda, J.; Gabsi, M. Vibrations and Acoustic Noise Analyses of Modular SPM Machines. In Proceedings of the 2020 IEEE Energy Conversion Congress and Exposition (ECCE), Detroit, MI, USA, 11–15 October 2020; pp. 5567–5573.
44. Le Besnerais, J. Effect of lamination asymmetries on magnetic vibrations and acoustic noise in synchronous machines. In Proceedings of the 2015 18th International Conference on Electrical Machines and Systems (ICEMS), Pattaya, Thailand, 25–28 October 2015; pp. 1729–1733.
45. Vandenbossche, L.; Jacobs, S.; Henrotte, F.; Hameyer, K. Impact of cut edges on magnetization curves and iron losses in e-machines for automotive traction. *World Electr. Veh. J.* **2010**, *4*, 587–596. [CrossRef]
46. Crevecoeur, G.; Sergeant, P.; Dupre, L.; Vandenbossche, L.; Van de Walle, R. Analysis of the Local Material Degradation Near Cutting Edges of Electrical Steel Sheets. *IEEE Trans. Magn.* **2008**, *44*, 3173–3176. [CrossRef]
47. Baker, N.J.; Smith, D.J.; Kulan, M.C.; Turvey, S. Design and performance of a segmented stator permanent magnet alternator for aerospace. In Proceedings of the 8th IET International Conference on Power Electronics, Machines and Drives (PEMD 2016), Glasgow, UK, 19–21 April 2016; pp. 1–6.
48. Vandenbossche, L.; Jacobs, S.; Van Hoecke, D.; Weber, B.; Leunis, E.; Attrazic, E. Improved iron loss modelling approach for advanced electrical steels operating at high frequencies and high inductions in automotive machines. In Proceedings of the 2012 2nd International Electric Drives Production Conference (EDPC), Nuremberg, Germany, 15–18 October 2012; pp. 1–8.
49. Dedulle, J.; Meunier, G.; Foggia, A.; Sabonnadiere, J.; Shen, D. Magnetic fields in nonlinear anisotropic grain-oriented iron-sheet. *IEEE Trans. Magn.* **1990**, *26*, 524–527. [CrossRef]
50. Lin, D.; Zhou, P.; Badics, Z.; Fu, W.; Chen, Q.; Cendes, Z. A new nonlinear anisotropic model for soft magnetic materials. *IEEE Trans. Magn.* **2006**, *42*, 963–966. [CrossRef]
51. Aggarwal, A. Analysis of PMSM Manufactured Using Segmented Stator Made from Oriented Steel. Ph.D. Thesis, Michigan State University, East Lansing, MI, USA, 2021.
52. Yang, R. Electrified Vehicle Traction Machine Design with Manufacturing Considerations. Ph.D. Thesis, McMaster University, Hamilton, ON, Canada, 2017.
53. Chen, Z.; Spooner, E. A modular, permanent-magnet generator for variable speed wind turbines. In Proceedings of the 1995 Seventh International Conference on Electrical Machines and Drives (Conf. Publ. No. 412), Durham, UK, 11–13 September 1995; pp. 453–457.
54. Du, Y.; Sun, Y.; Zhu, X.; Cheng, M.; Xiao, F.; Sun, Y.; Zhu, H. Comparison of doubly salient permanent magnet machines with E-shaped and π-shaped stator iron core segments. In Proceedings of the 2015 IEEE International Magnetics Conference (INTERMAG), Beijing, China, 11–15 May 2015; p. 1.
55. Segmented Stator & Rotor Lamination in China. Available online: https://motorneo.com/segment-motor-core/# (accessed on 1 July 2024).

56. JYSTATOR. What Is Stator Bonding Lamination Technology and How to Do It. Available online: https://www.jystator.com/Statorbonding.html#_np=150_505 (accessed on 1 July 2024).
57. Arshad, W.M.; Ryckebush, T.; Magnussen, F.; Lendenmann, H.; Soulard, J.; Eriksson, B.; Malmros, B. Incorporating Lamination Processing and Component Manufacturing in Electrical Machine Design Tools. In Proceedings of the 2007 IEEE Industry Applications Annual Meeting, New Orleans, LA, USA, 23–27 September 2007; pp. 94–102.
58. Sheeran, K.A.; Rassoolkhani, P.; Michaels, P.G. Segmented Stator with Improved Handling and Winding Characteristics. U.S. Patent 7471025-B2, 30 December 2008.
59. Shen, J.X.; Cai, S.; Yuan, J.; Cao, S.; Shi, C.W. Cogging torque in SPM machine with segmented stator. *COMPEL-Int. J. Comput. Math. Electr. Electron. Eng.* **2015**, *35*, 641–654. [CrossRef]
60. Yuan, J.; Shi, C.W.; Shen, J.X. Analysis of cogging torque in surface-mounted permanent magnet machines with segmented stators. In Proceedings of the 2014 17th International Conference on Electrical Machines and Systems (ICEMS), Hangzhou, China, 22–25 October 2014; pp. 2513–2516.
61. Stator Segmentation: Material Savings and CO_2 Reduction. Available online: https://www.swd-technology.com/en/technologies/stator-segmentation/ (accessed on 1 July 2024).
62. Mecrow, B.; Finch, J.; El-Kharashi, E.; Jack, A. Switched reluctance motors with segmental rotors. *IEE Proc.-Electr. Power Appl.* **2002**, *149*, 245–254. [CrossRef]
63. Dong, J.; Huang, Y.; Jin, L.; Lin, H. Comparative Study of Surface-Mounted and Interior Permanent-Magnet Motors for High-Speed Applications. *IEEE Trans. Appl. Supercond.* **2016**, *26*, 1–4. [CrossRef]
64. Zulu, A.; Mecrow, B.C.; Armstrong, M. Permanent-Magnet Flux-Switching Synchronous Motor Employing a Segmental Rotor. *IEEE Trans. Ind. Appl.* **2012**, *48*, 2259–2267. [CrossRef]
65. Schoppa, A.; Schneider, J.; Wuppermann, C.D. Influence of the manufacturing process on the magnetic properties of non-oriented electrical steels. *J. Magn. Magn. Mater.* **2000**, *215–216*, 74–78. [CrossRef]
66. Baker, N.J.; Smith, D.J.B.; Kulan, M.C.; Turvey, S. Design and Performance of a Segmented Stator Permanent Magnet Alternator for Aerospace. *IEEE Trans. Energy Convers.* **2018**, *33*, 40–48. [CrossRef]
67. Staeuble, T. Differences in Bonding Technology Explained. 2023. Available online: https://www.swd-technology.com/en/differences-in-bonding-technology-explained/ (accessed on 1 July 2024).
68. Lee, S.W. Laminated Body Of Motor And Manufacturing Method Thereof. U.S. Patent 7271519-B2, 18 September 2007.
69. Vandenbossche, L.; Jacobs, S.; Van Hoecke, D.; Attrazic, E. Impact of mechanical stresses on the magnetic performance of non-oriented electrical steels and its relation to electric machine efficiency. In Proceedings of the 2015 IEEE Transportation Electrification Conference and Expo (ITEC), Dearborn, MI, USA, 14–17 June 2015; pp. 1–6.
70. Brettschneider, J.; Spitzner, R.; Boehm, R. Flexible mass production concept for segmented BLDC stators. In Proceedings of the 2013 3rd International Electric Drives Production Conference (EDPC), Nuremberg, Germany, 29–30 October 2013; pp. 1–8.
71. Kreidler, J.J.; Anderson, W.K.; Venkateswararao, S.; Conway, B.J.; Willis, H.D.; Wung, P.Y.P. Roll up stator development for 56 frame PM synchronous motor. In Proceedings of the 2014 IEEE Energy Conversion Congress and Exposition (ECCE), Pittsburgh, PA, USA, 14–18 September 2014; pp. 5571–5578.
72. Hoffman, M.D.; Mantey, R.J.; Sudhoff, D.H.; Mazza, L.; Paxton, B.L.; Davis, J.L.; Dorsch, D.S. Segmented Stator Assembly. U.S. Patent 9343930-B2, 17 May 2016.
73. NIDE Group. Stator Spiral Winding Slinky Production Machine. Available online: https://www.nide-group.com/En/pro_detail/mid/39/id/186.html (accessed on 1 July 2024).
74. Xu, F.; Zhu, Z.Q.; He, T.R.; Wang, Y.; Bin, H.; Wu, D.; Gong, L.M.; Chen, J.T. Influence of Stator Gap on Electromagnetic Performance of 6-Slot/2-Pole Modular High Speed Permanent Magnet Motor with Toroidal Windings. *IEEE Access* **2021**, *9*, 94470–94494. [CrossRef]
75. Aggarwal, A.; Meier, M.; Strangas, E.; Agapiou, J. Analysis of Modular Stator PMSM Manufactured Using Oriented Steel. *Energies* **2021**, *14*, 6583. [CrossRef]
76. Momen, M.F.; Datta, S. Analysis of Flux Leakage in a Segmented Core Brushless Permanent Magnet Motor. *IEEE Trans. Energy Convers.* **2009**, *24*, 77–81. [CrossRef]
77. Petrov, I.; Di, C.; Lindh, P.; Niemelä, M.; Repo, A.K.; Pyrhönen, J. Fault-Tolerant Modular Stator Concentrated Winding Permanent Magnet Machine. *IEEE Access* **2020**, *8*, 7806–7816. [CrossRef]
78. Dajaku, G. Electrical Machine. U.S. Patent 0316368 A1, 29 December 2011.
79. Dajaku, G.; Gerling, D. A novel 12-teeth/10-poles PM machine with flux barriers in stator yoke. In Proceedings of the 2012 XXth International Conference on Electrical Machines, Marseille, France, 2–5 September 2012; pp. 36–40.
80. Li, G.J.; Zhu, Z.Q.; Foster, M.; Stone, D. Comparative Studies of Modular and Unequal Tooth PM Machines Either With or Without Tooth Tips. *IEEE Trans. Magn.* **2014**, *50*, 1–10. [CrossRef]
81. Dajaku, G.; Gerling, D. Low costs and high-efficiency electric machines. In Proceedings of the 2012 2nd International Electric Drives Production Conference (EDPC), Nuremberg, Germany, 15–18 October 2012; pp. 1–7.

82. Bilyi, V.; Gerling, D. Design of high-efficiency interior permanent magnet synchronous machine with stator flux barriers and single-layer concentrated windings. In Proceedings of the 2015 IEEE International Electric Machines & Drives Conference (IEMDC), Coeur d'Alene, ID, USA, 10–13 May 2015; pp. 1177–1183.
83. Zhang, W.; Li, G.J.; Zhu, Z.Q.; Ren, B.; Michon, M. Optimization of Modular SPM Machines Considering Stator Modularity. In Proceedings of the 2021 IEEE International Electric Machines & Drives Conference (IEMDC), Hartford, CT, USA, 17–20 May 2021; pp. 1–6.
84. Gerold, J.W.; Gerling, D. An equivalent winding factor larger than 1 by using flux barriers in the stator. In Proceedings of the 2019 IEEE International Electric Machines & Drives Conference (IEMDC), San Diego, CA, USA, 12–15 May 2019; pp. 1855–1862.
85. Gerold, J.W.; Gerling, D. Analysis of Different Arrangements of Flux Barriers and Different Pole Pairs in a Stator with Concentrated Winding. In Proceedings of the 2018 XIII International Conference on Electrical Machines (ICEM), Alexandroupoli, Greece, 3–6 September 2018; pp. 58–64.
86. Gerold, J.W.; Gerling, D. Design rules for Stators with Flux Barriers. In Proceedings of the 2019 IEEE 13th International Conference on Power Electronics and Drive Systems (PEDS), Toulouse, France, 9–12 July 2019; pp. 1–8.
87. Gerold, J.W.; Lu, F.; Gerling, D. An Additional Short-Circuited Stator Winding in Flux-Barriers to Improve the Machine Performance. In Proceedings of the 2020 23rd International Conference on Electrical Machines and Systems (ICEMS), Hamamatsu, Japan, 24–27 November 2020; pp. 565–570.
88. Dajaku, G.; Roth, C. Comparison Study of Different FSCWs with Flux Barrier Stator. In Proceedings of the 2023 IEEE International Electric Machines & Drives Conference (IEMDC), San Francisco, CA, USA, 15–18 May 2023; pp. 1–6.
89. Khoshoo, B.; Aggarwal, A.; Barron, M.; Foster, S.N. Analysis of Segmented Stator and Rotor Design in PMSM Using A Physics-Based MEC Model. In Proceedings of the 2024 IEEE Energy Conversion Congress and Exposition (ECCE), Phoenix, AZ, USA, 20–24 October 2024.
90. Mecrow, B.; El-Kharashi, E.; Finch, J.; Jack, A. Preliminary performance evaluation of switched reluctance motors with segmental rotors. *IEEE Trans. Energy Convers.* **2004**, *19*, 679–686. [CrossRef]
91. Oyama, J.; Higuchi, T.; Abe, T.; Tanaka, K. The fundamental characteristics of novel switched reluctance motor with segment core embedded in aluminum rotor block. In Proceedings of the 2005 International Conference on Electrical Machines and Systems, Nanjing, China, 27–29 September 2005; Volume 1, pp. 515–519.
92. Vattikuti, N.; Rallabandi, V.; Fernandes, B.G. A novel high torque and low weight segmented switched reluctance motor. In Proceedings of the 2008 IEEE Power Electronics Specialists Conference, Rhodes, Greece, 15–19 June 2008; pp. 1223–1228.
93. Kabir, M.A.; Husain, I. Segmented rotor design of concentrated wound switched reluctance motor (SRM) for torque ripple minimization. In Proceedings of the 2016 IEEE Energy Conversion Congress and Exposition (ECCE), Milwaukee, WI, USA, 18–22 September 2016; pp. 1–6.
94. Loh, J.Y.; Prabhu, M.A.; Wang, S.; Joshi, S.C.; Viswanathan, V.; Ramakrishna, S. Optimal segmented rotor design for the embedded electrical machine for the more electric aircraft. *J. Eng.* **2019**, *2019*, 4321–4324. [CrossRef]
95. Nikam, S.P.; Rallabandi, V.; Fernandes, B.G. A High-Torque-Density Permanent-Magnet Free Motor for in-Wheel Electric Vehicle Application. *IEEE Trans. Ind. Appl.* **2012**, *48*, 2287–2295. [CrossRef]
96. Rallabandi, V.; Han, P.; Wu, J.; Cramer, A.M.; Ionel, D.M.; Zhou, P. Design Optimization and Comparison of Direct-Drive Outer-Rotor SRMs Based on Fast Current Profile Estimation and Transient FEA. *IEEE Trans. Ind. Appl.* **2021**, *57*, 236–245. [CrossRef]
97. Mousavi-Aghdam, S.R.; Feyzi, M.R.; Bianchi, N.; Morandin, M. Design and Analysis of a Novel High-Torque Stator-Segmented SRM. *IEEE Trans. Ind. Electron.* **2016**, *63*, 1458–1466. [CrossRef]
98. Lian, G.; Gu, G.; Cheng, Y.; Tao, J.; Wang, S.; Chen, X. Comparative study on switched reluctance and flux-switching machines with segmental rotors. In Proceedings of the 2015 18th International Conference on Electrical Machines and Systems (ICEMS), Pattaya, Thailand, 25–28 October 2015; pp. 845–848.
99. Zhu, Z.Q.; Chen, J.T.; Pang, Y.; Howe, D.; Iwasaki, S.; Deodhar, R. Analysis of a Novel Multi-Tooth Flux-Switching PM Brushless AC Machine for High Torque Direct-Drive Applications. *IEEE Trans. Magn.* **2008**, *44*, 4313–4316. [CrossRef]
100. Andrada, P.; Blanqué, B.; Martínez, E.; Torrent, M. New hybrid reluctance motor drive. In Proceedings of the 2012 XXth International Conference on Electrical Machines, Marseille, France, 2–5 September 2012; pp. 2689–2694.
101. Ullah, S.; McDonald, S.P.; Martin, R.; Benarous, M.; Atkinson, G.J. A Permanent Magnet Assist, Segmented Rotor, Switched Reluctance Drive for Fault Tolerant Aerospace Applications. *IEEE Trans. Ind. Appl.* **2019**, *55*, 298–305. [CrossRef]
102. Ionel, D.; Eastham, J.; Betzer, T. Finite element analysis of a novel brushless DC motor with flux barriers. *IEEE Trans. Magn.* **1995**, *31*, 3749–3751. [CrossRef]
103. Ionel, D.; Balchin, M.; Eastham, J.; Demeter, E. Finite element analysis of brushless DC motors for flux weakening operation. *IEEE Trans. Magn.* **1996**, *32*, 5040–5042. [CrossRef]

104. Bianchi, N.; Bolognani, S. Performance analysis of an IPM motor with segmented rotor for flux-weakening applications. In Proceedings of the 1999 Ninth International Conference on Electrical Machines and Drives (Conf. Publ. No. 468), Canterbury, UK, 1–3 September 1999; pp. 49–53.
105. Bianchi, N.; Bolognani, S.; Chalmers, B. Salient-rotor PM synchronous motors for an extended flux-weakening operation range. *IEEE Trans. Ind. Appl.* **2000**, *36*, 1118–1125. [CrossRef]
106. Fontana, M.; Bianchi, N. Design and Analysis of Normal Saliency IPM Spoke Motor. *IEEE Trans. Ind. Appl.* **2020**, *56*, 3625–3635. [CrossRef]
107. Khoshoo, B.; Madovi, O.; Aggarwal, A.; Foster, S.N. Impact of Rotor Segmentation on Electromagnetic Performance of PM Machine. In Proceedings of the 2022 International Conference on Electrical, Computer and Energy Technologies (ICECET), Prague, Czech Republic, 20–22 July 2022; pp. 1–7.
108. EL-Refaie, A.M.; Alexander, J.P.; Galioto, S.; Reddy, P.B.; Huh, K.K.; de Bock, P.; Shen, X. Advanced High-Power-Density Interior Permanent Magnet Motor for Traction Applications. *IEEE Trans. Ind. Appl.* **2014**, *50*, 3235–3248. [CrossRef]
109. Cirani, M.; Eriksson, S.; Thunberg, J. Innovative Design for Flux Leakage Reduction in IPM Machines. *IEEE Trans. Ind. Appl.* **2014**, *50*, 1847–1853. [CrossRef]
110. Li, J.; Wang, K.; Zhang, H. Flux-Focusing Permanent Magnet Machines with Modular Consequent-Pole Rotor. *IEEE Trans. Ind. Electron.* **2020**, *67*, 3374–3385. [CrossRef]
111. Live, M. Tesla Model S Plaid Motor EXTRAVAGANZA!! 2022. Available online: https://www.youtube.com/watch?v=4lGVimLK58g&t=900s (accessed on 1 July 2024).
112. Boglietti, A.; Cavagnino, A.; Lazzari, M.; Pastorelli, M. Effects of punch process on the magnetic and energetic properties of soft magnetic material. In Proceedings of the IEMDC 2001. IEEE International Electric Machines and Drives Conference (Cat. No. 01EX485), Cambridge, MA, USA, 17–20 June 2001; pp. 396–399.
113. Nakata, T.; Nakano, M.; Kawahara, K. Effects of Stress Due to Cutting on Magnetic Characteristics of Silicon Steel. *IEEE Transl. J. Magn. Jpn.* **1992**, *7*, 453–457. [CrossRef]
114. Baudouin, P.; De Wulf, M.; Kestens, L.; Houbaert, Y. The effect of the guillotine clearance on the magnetic properties of electrical steels. *J. Magn. Magn. Mater.* **2003**, *256*, 32–40. [CrossRef]
115. Lee, H.; Park, J.T. Effect of Cut-Edge Residual Stress on Magnetic Properties in Non-Oriented Electrical Steel. *IEEE Trans. Magn.* **2019**, *55*, 1–4. [CrossRef]
116. Weiss, H.A.; Tröber, P.; Golle, R.; Steentjes, S.; Leuning, N.; Elfgen, S.; Hameyer, K.; Volk, W. Impact of Punching Parameter Variations on Magnetic Properties of Nongrain-Oriented Electrical Steel. *IEEE Trans. Ind. Appl.* **2018**, *54*, 5869–5878. [CrossRef]
117. *IEC 60404-2:1996*; Magnetic Materials—Part 2: Methods of Measurement of the Magnetic Properties of Electrical Steel Sheet and Strip by Means of an Epstein Frame. IEC: Geneva, Switzerland, 1996.
118. *IEC 60404-10:2016*; Magnetic Materials—Part 10: Methods of Measurement of Magnetic Properties of Electrical Steel Strip and Sheet at Medium Frequencies. IEC: Geneva, Switzerland, 2016.
119. Moses, A.; Derebasi, N.; Loisos, G.; Schoppa, A. Aspects of the cut-edge effect stress on the power loss and flux density distribution in electrical steel sheets. *J. Magn. Magn. Mater.* **2000**, *215–216*, 690–692. [CrossRef]
120. Omura, T.; Zaizen, Y.; Fukumura, M.; Senda, K.; Toda, H. Effect of Hardness and Thickness of Nonoriented Electrical Steel Sheets on Iron Loss Deterioration by Shearing Process. *IEEE Trans. Magn.* **2015**, *51*, 1–4. [CrossRef]
121. Ossart, F.; Hug, E.; Hubert, O.; Buvat, C.; Billardon, R. Effect of punching on electrical steels: Experimental and numerical coupled analysis. *IEEE Trans. Magn.* **2000**, *36*, 3137–3140. [CrossRef]
122. Pulnikov, A.; Baudouin, P.; Melkebeek, J. Induced stresses due to the mechanical cutting of non-oriented electrical steels. *J. Magn. Magn. Mater.* **2003**, *254–255*, 355–357. [CrossRef]
123. Senda, K.; Ishida, M.; Nakasu, Y.; Yagi, M. Influence of shearing process on domain structure and magnetic properties of non-oriented electrical steel. *J. Magn. Magn. Mater.* **2006**, *304*, e513–e515. [CrossRef]
124. Slota, J.; Spišák, E.; Kaščák, L.; Majerníková, J. Experimental and finite element analysis of the shear cutting process of electrical steel sheets under various process conditions. *IOP Conf. Ser. Mater. Sci. Eng.* **2019**, *651*, 012084. [CrossRef]
125. Wu, F.; Zhou, L.; Soulard, J.; Silvester, B.; Davis, C. Quantitative characterisation and modelling of the effect of cut edge damage on the magnetic properties in NGO electrical steel. *J. Magn. Magn. Mater.* **2022**, *551*, 169185. [CrossRef]
126. Gmyrek, Z.; Cavagnino, A.; Ferraris, L. Estimation of the Magnetic Properties of the Damaged Area Resulting From the Punching Process: Experimental Research and FEM Modeling. *IEEE Trans. Ind. Appl.* **2013**, *49*, 2069–2077. [CrossRef]
127. Gmyrek, Z.; Cavagnino, A. Analytical Model of the Ferromagnetic Properties in Laminations Damaged by Cutting. In Proceedings of the 2021 IEEE Energy Conversion Congress and Exposition (ECCE), Vancouver, BC, Canada, 10–14 October 2021; pp. 4000–4007.
128. Fujisaki, K.; Hirayama, R.; Kawachi, T.; Satou, S.; Kaidou, C.; Yabumoto, M.; Kubota, T. Motor Core Iron Loss Analysis Evaluating Shrink Fitting and Stamping by Finite-Element Method. *IEEE Trans. Magn.* **2007**, *43*, 1950–1954. [CrossRef]
129. Kaido, C. Mechanical method of iron loss measurement in a rotational field and analysis of iron loss in a motor. *J. Appl. Phys.* **1991**, *69*, 5106–5108. [CrossRef]

130. Vandenbossche, L.; Jacobs, S.; Jannot, X.; McClelland, M.; Saint-Michel, J.; Attrazic, E. Iron loss modelling which includes the impact of punching, applied to high-efficiency induction machines. In Proceedings of the 2013 3rd International Electric Drives Production Conference (EDPC), Nuremberg, Germany, 29–30 October 2013; pp. 1–10.
131. Bali, M.; De Gersem, H.; Muetze, A. Finite-Element Modeling of Magnetic Material Degradation Due to Punching. *IEEE Trans. Magn.* **2014**, *50*, 745–748. [CrossRef]
132. Elfgen, S.; Steentjes, S.; Böhmer, S.; Franck, D.; Hameyer, K. Continuous Local Material Model for Cut Edge Effects in Soft Magnetic Materials. *IEEE Trans. Magn.* **2016**, *52*, 1–4. [CrossRef]
133. Goldbeck, G.; Cossale, M.; Kitzberger, M.; Bramerdorfer, G.; Andessner, D.; Amrhein, W. Incorporating the Soft Magnetic Material Degradation to Numerical Simulations. *IEEE Trans. Ind. Appl.* **2020**, *56*, 3584–3593. [CrossRef]
134. Mohammadi, A.A.; Zhang, S.; Pop, A.C.; Gyselinck, J.J.C. Effect of Electrical Steel Punching on the Performance of Fractional-kW Electrical Machines. *IEEE Trans. Energy Convers.* **2022**, *37*, 1854–1863.
135. Breining, P.; Rollbühler, C.; Sjöberg, L.; Doppelbauer, M. Magnetic Characterization of Stator Segments made of Soft Magnetic Composites. In Proceedings of the 2020 International Conference on Electrical Machines (ICEM), Gothenburg, Sweden, 23–26 August 2020; pp. 2307–2313.
136. Breining, P.; Doppelbauer, M. Magnetic Characterization of Stator Segments Considering Mechanical Stress. In Proceedings of the 2022 International Conference on Electrical Machines (ICEM), Valencia, Spain, 5–8 September 2022; pp. 2155–2161.
137. Khoshoo, B.; Aggarwal, A.; Agapiou, J.; Foster, S.N. Experimental Evaluation of the Impact of Using Oriented Steel in Proportion to Segmentation on Core Loss of AC Electric Machine Stator. In Proceedings of the 2024 IEEE Energy Conversion Congress and Exposition (ECCE), Phoenix, AZ, USA, 20–24 October 2024.
138. Nencib, N.; Spornic, S.; Kedous-Lebouc, A.; Cornut, B. Macroscopic anisotropy characterization of SiFe using a rotational single sheet tester. *IEEE Trans. Magn.* **1995**, *31*, 4047–4049. [CrossRef]
139. Lopez, S.; Cassoret, B.; Brudny, J.F.; Lefebvre, L.; Vincent, J.N. Grain Oriented Steel Assembly Characterization for the Development of High Efficiency AC Rotating Electrical Machines. *IEEE Trans. Magn.* **2009**, *45*, 4161–4164. [CrossRef]
140. Cassoret, B.; Lopez, S.; Brudny, J.F.; Belgrand, T. Non-Segmented Grain Oriented Steel in Induction Machines. *Prog. Electromagn. Res. C* **2014**, *47*, 1–10. [CrossRef]
141. Mallard, V.; Parent, G.; Demian, C.; Brudny, J.F.; Delamotte, A. Increasing the energy-efficiency of induction machines by the use of grain oriented magnetic materials and die-casting copper squirrel cage in the rotor. In Proceedings of the 2017 IEEE International Electric Machines and Drives Conference (IEMDC), Miami, FL, USA, 21–24 May 2017; pp. 1–6.
142. Kaneki, O.; Higuchi, T.; Yokoi, Y.; Abe, T.; Miyamoto, Y.; Ohto, M. Performance of segment type switched reluctance motor using grain-oriented. In Proceedings of the 2012 15th International Conference on Electrical Machines and Systems (ICEMS), Sapporo, Japan, 21–24 October 2012; pp. 1–4.
143. Pei, R.; Zeng, L.; Li, S.; Coombs, T. Studies on grain-oriented silicon steel used in traction motors. In Proceedings of the 2017 20th International Conference on Electrical Machines and Systems (ICEMS), Sydney, NSW, Australia, 11–14 August 2017; pp. 1–5.
144. Yu, Y.; Hao, Z.; Bi, Y.; Pei, Y. Performance analysis between Grain-oriented and Non-oriented Material on Yokeless And Segmented Armature Machine. In Proceedings of the 2019 22nd International Conference on Electrical Machines and Systems (ICEMS), Harbin, China, 11–14 August 2019; pp. 1–5.
145. Kowal, D.; Sergeant, P.; Dupre, L.; Van den Bossche, A. Comparison of Nonoriented and Grain-Oriented Material in an Axial Flux Permanent-Magnet Machine. *IEEE Trans. Magn.* **2010**, *46*, 279–285. [CrossRef]
146. Taghavi, S.; Pillay, P. A Novel Grain-Oriented Lamination Rotor Core Assembly for a Synchronous Reluctance Traction Motor with a Reduced Torque Ripple Algorithm. *IEEE Trans. Ind. Appl.* **2016**, *52*, 3729–3738. [CrossRef]
147. Munteanu, A.; Nastas, I.; Simion, A.; Livadaru, L.; Virlan, B.; Nacu, I. A New Topology of Fractional-Slot ConcentratedWound Permanent Magnet Synchronous Motor with Grain-Oriented Electric Steel for Stator Laminations. In Proceedings of the 2021 International Conference on Electromechanical and Energy Systems (SIELMEN), Iasi, Romania, 6–8 October 2021; pp. 349–352.
148. Enokizono, M. Two-dimensional (vector) magnetic property and improved magnetic field analysis for electrical machines. *J. Mater. Process. Technol.* **2001**, *108*, 225–231. [CrossRef]
149. Liu, J.; Basak, A.; Moses, A.; Shirkoohi, G. A method of anisotropic steel modelling using finite element method with confirmation by experimental results. *IEEE Trans. Magn.* **1994**, *30*, 3391–3394. [CrossRef]
150. Soda, N.; Enokizono, M. E&S hysteresis model for two-dimensional magnetic properties. *Journal of Magnetism and Magnetic Materials* **2000**, *215–216*, 626–628.
151. Enokizono, M. Vector Magnetic Property and Magnetic Characteristic Analysis by Vector Magneto-Hysteretic E&S Model. *IEEE Trans. Magn.* **2009**, *45*, 1148–1153.
152. Soda, N.; Enokizono, M. Utilization method of electrical steel sheets on stator of self-propelled rotary actuator. In Proceedings of the 2016 XXII International Conference on Electrical Machines (ICEM), Lausanne, Switzerland, 4–7 September 2016; pp. 918–923.

153. Tolmachev, S.; Il'chenko, O. Mathematical modelling of magnetic properties of non-linear anisotropic medium in anhysteretic approximation. In Proceedings of the 2017 International Conference on Modern Electrical and Energy Systems (MEES), Kremenchuk, Ukraine, 15–17 November 2017; pp. 316–319.
154. Li, Z.; Ma, Y.; Hu, A.; Zeng, L.; Xu, S.; Pei, R. Investigation and Application of Magnetic Properties of Ultra-Thin Grain-Oriented Silicon Steel Sheets under Multi-Physical Field Coupling. *Materials* **2022**, *15*, 8522. [CrossRef] [PubMed]
155. Aggarwal, A.; Khoshoo, B.; Agapiou, J.; Foster, S.N. A More Accurate FEA Model for Machines with Segmented Stators Manufactured using Oriented Steel. In Proceedings of the 2024 IEEE Energy Conversion Congress and Exposition (ECCE), Phoenix, AZ, USA, 20–24 October 2024.